Modeling and Experimental Studies of SO_2 Effects on CO_2 Capture with Chilled Ammonia Solvent

by

Kuang Cheng

A thesis

presented to the University of Waterloo

in fulfillment of the

thesis requirement for the degree of

Master of Applied Science

in

Chemical Engineering

Waterloo, Ontario, Canada, 2016

AUTHOR'S DECLARATION

I hereby declare that I am the sole author of this thesis. This is a true copy of the thesis, including any required final revisions, as accepted by my examiners.

I understand that my thesis may be made electronically available to the public.

Abstract

Combustion of fossil fuel produces air emissions including carbon dioxide, nitric oxide, and sulfur dioxide, which cause severe environment problems, in particular, global warming and environmental pollution. The discharge of the power plant is the primary source of carbon dioxide emission. For CO_2 capture from existing plants, the post-combustion carbon capture is the most widely used technology because of the lower cost to retrofit the plant. Chilled ammonia has been reported as an absorbent in post-combustion carbon capture, which shows low energy cost and high efficiency.

Although carbon dioxide is usually captured after desulfurization and denitrification of the flue gas, such processes can hardly remove the entire sulfur dioxide. Sulfur dioxide is known to have a negative effect on carbon dioxide capture.

In this study, the effect of sulfur dioxide on carbon dioxide mass transfer was investigated. Chilled ammonium water was used as absorbent. The experimental data confirms the negative effects of sulfur dioxide on carbon dioxide capture using chilled ammonia. The mass transfer of carbon dioxide decreased with increasing concentration of sulfur dioxide in the gas phase. Numerical modeling of mass transfer of carbon dioxide in the presence of sulfur dioxide was developed and validated experimentally to better understand the effect of sulfur dioxide on carbon dioxide absorption by aqueous ammonia. In this work, an assumed reaction plane was introduced to explain the sulfur dioxide effect on carbon dioxide mass transfer into aqueous ammonia. For easiness of using the model to estimate the effect of sulfur dioxide, a general equation was also developed by fitting the numerical solutions. The concentration of carbon dioxide reacted with aqueous ammonia is lower than the equilibrium concentration of carbon dioxide in the gas-liquid interface. The main outcome was the quantification of the concentration of carbon dioxide in the reaction plane (C_r) as a function of partial pressure of SO_2 in the gas phase (S_0) and equilibrium concentration of carbon dioxide in the liquid surface (C_0) with various aqueous ammonia concentration (C_{NH_3}); this relationship is as follows:

$$C_r = \left(1 + \left(-2.92744 + 1.75\left(1 - \exp\left(-\frac{C_{NH_3}}{0.6213}\right)\right)\right) S_0 \times 10^{-4} + 1.2525 \times 10^{-8} {S_0}^2\right) C_0$$

Acknowledgements

Foremost, I would like to thank my co-supervisors Drs. Zhongchao Tan and Eric Croiset for their directions and encouragement with this thesis. Their advice ensures the smooth progress of completing my thesis.

I also would like to acknowledge my thesis readers Drs. Xianshe Feng and Soo Jeon for their comments to improve the quality of the thesis on the numerical modeling part of this thesis.

I would like to acknowledge Dr. Jingde Li for his help in writing the numerical calculation program. Special thanks to Dr. Hesheng Yu for his help on using FTIR and others experimental instruments and Dr. Zhu for his help in data collection.

I would like to acknowledge financial support from the Ontario-China Research and Innovation Fund (OCRIF 2014).

Most importantly, I would express my gratitude to my family and my friends who encouraged and supported me through my degree.

Dedication

This dedication to my parents and my wife, Tianqing Zhang

Table of Contents

List of Symbols

Notation	Term	Unit
C	concentration	$mol \cdot L^{-1}$
C^*	liquid-phase concentration that would be in equilibrium with the bulk gas concentration	$mol \cdot L^{-1}$
C_b	concentration in bulk	$mol \cdot L^{-1}$
C_i	concentration at interface	$mol \cdot L^{-1}$
C_{lb}	concentration of carbon dioxide in bulk liquid	$mol \cdot L^{-1}$
C_{li}	equilibrium concentration of carbon dioxide in liquid interface	$mol \cdot L^{-1}$
D	molecular diffusivity of solute gas in liquid phase	$m^2 \cdot s^{-1}$
D_{CO_2}	diffusion coefficient of carbon dioxide in aqueous ammonia	$m^2 \cdot s^{-1}$
D_{SO_2}	diffusion coefficient of sulfur dioxide in aqueous ammonia	$m^2 \cdot s^{-1}$
D_{NH_3}	diffusion coefficient of ammonia in water	$m^2 \cdot s^{-1}$
D_L	diffusion coefficient for liquid phase	$m^2 \cdot s^{-1}$
E	enhancement factor	-
H	Henry's constant	$L \cdot pa \cdot mol^{-1}$
H_c	Henry's constant for carbon dioxide	$L \cdot pa \cdot mol^{-1}$

J	flux of species	$m^{-2}·s^{-1}$
k	reaction rate constant	$L·mol^{-1}$
k_{OH^-}	reaction rate constant of carbon dioxide and hydroxide ions in reaction (R 4-3)	L·mol-1
K	equilibrium constant for specific reaction	-
k_{obs}	obvious reaction rate constant	s^{-1}
k_{app}	apparent reaction rate constant	s^{-1}
k_{f1}	second order reaction rate constant of reaction (R 4-1)	m^3mol^{-1} s^{-1}
k_G	gas-phase mass transfer coefficient	$mol·s^{-1}·m^{-2}$ pa^{-1}
K_G	overall mass transfer coefficient based on gas-phase concentration.	$mol·s^{-1}·m^{-2}$ pa^{-1}
k_L	liquid-phase mass transfer coefficient	$m·s^{-1}$
K_L	overall mass transfer coefficient based on liquid-phase concentration	$m·s^{-1}$
$K_{overall}$	overall reaction rate constant	s^{-1}
M	molecular weight	g
n	mass amount of species of gas	mol
n_L	liquid-phase stirring speed	rpm

N	molar flux of species per unit area per unit time	$mol \cdot L \cdot s^{-1}$
N_{CO_2}	molar mass flux of carbon dioxide	$mol \cdot L \cdot s^{-1}$
P	partial pressure of species in gas phase under equilibrium condition	pa
P^*	gas-phase concentration that would be in equilibrium with the bulk liquid concentration	pa
P_{gb}	partial pressure of carbon dioxide in bulk gas	pa
P_{gi}	partial pressure of carbon dioxide in gas interface	pa
Q	volumetric flow rate of species	$L \cdot s^{-1}$
r	reaction rate	$mol \cdot L^{-1} \cdot s^{-1}$
$r_{overall}$	overall reaction rate for CO_2 absorption	$mol \cdot L^{-1} \cdot s^{-1}$
$r_{CO_2-NH_3}$	reaction rate of carbon dioxide and ammonia by equation (4-40)	$mol \cdot L^{-1} \cdot s^{-1}$
$r_{forward}$	forward reaction rate of carbamate formation (R 4-1)	$mol \cdot L^{-1} \cdot s^{-1}$
$r_{backward}$	backward reaction rate of carbamate decomposition	$mol \cdot L^{-1} \cdot s^{-1}$
R	universal gas constant	$8.314 J \cdot mol^{-1} \cdot k^{-1}$
S	area of interface	m^2
T	temperature	K

V	volume of the gas	L
v	velocity of mass flux	$m \cdot s^{-1}$
V_b	molar volume of species at its normal boiling temperature	$cm^3 \cdot mol^{-1}$
X	length of flux through a direction	m
x_r	distance from interface to reaction plane	m
x_f	thickness of the stagnate film	m

Greek letters

γ	association parameter	-
δ	thickness of stagnant film	m
δ_L	thickness of liquid film	m
μ	viscosity	Pa·s

Dimensionless groups

$c = \frac{C_{CO_2}}{C_0}$	dimensionless carbon dioxide concentration
$a = \frac{C_{NH_3}}{C_{NH_3}^0}$	dimensionless ammonia concentration

$\xi = \frac{x}{x_f}$ dimensionless length

$\omega = \frac{k_{CO_2-NH_3} C_0 {x_f}^2}{\mathrm{D}_{CO_2-NH_3}}$ dimensionless ratio of reaction and diffusion rate

$r_{SO_2} = \frac{\mathrm{D}_{SO_2-NH_3}}{\mathrm{D}_{CO_2-NH_3}}$ dimensionless diffusion coefficient of sulfur dioxide

$p = \frac{k_{SO_2-NH_3}}{k_{CO_2-NH_3}}$ dimensionless reaction rate constant

$s = \frac{C_{SO_2}}{S_0}$ dimensionless concentration of sulfur dioxide

$r_{NH_3} = \frac{\mathrm{D}_{NH_3-H_2O}}{\mathrm{D}_{CO_2-NH_3}}$ dimensionless diffusion coefficient of ammonia

List of Figures

Chapter 1 Introduction

1.1 Research Motivations

CO_2 is one of the major greenhouse gases. Excessive greenhouse gases in the atmosphere are believed to be responsible for various environmental problems like the continuous rise of sea level, the increasing number of ocean storms, floods, and others. Emissions from the fossil fuel powers plant are the primary source of carbon dioxide emissions[1]. Technologies for carbon dioxide capture from power plants include pre-combustion carbon capture, oxy-fuel combustion, and post-combustion carbon capture[2]. Because of the low cost of modifying existing facilities, the post-combustion carbon capture is the most widely used technology[3]. Among post-combustion capture techniques, solvent-based technologies are the most mature technologies.

However, one challenge to the absorption of CO_2 is the deleterious effects of sulfur dioxide in the flue gas even after flue gas desulfurization (FGD) process[4]. As reported by Dhegihan[5], the desulfurization efficiencies of absorption and adsorption are 90–98% and 50–60% SO_2 , respectively. For a typical coal-fired power plant of 300 MW using coal with 1.2% sulfur content, the flue gas stream from combustion chamber contains about 300 ppm SO_2 after wet desulfurization[6].

As an alternative to the conventional amine-based process, chilled ammonia process is a promising alternate post-combustion carbon capture process[7]. In particular, chilled ammonia process has a potential to address the high energy cost of carbon dioxide regeneration in traditional amine-based systems[7]. Such a process requires lowering the flue gas temperature to 0-20°C in order to maximize the absorption efficiency of CO_2 chilled by ammonia. Regeneration is accomplished by increasing the pressure and temperature downstream of the CO_2 absorber. High-pressure CO_2 vapor formed the pressurized stream.

The method shows lower energy consumption and low volatilization of ammonia. However, the effects of the sulfur dioxide need to be investigated. Qi et al. have studied the effects of SO_2 on CO_2 mass transfer with aqueous ammonia in the temperature range 20-80°C using a falling film reactor. They did not consider low temperatures (0-20°C). The effects of sulfur dioxide on carbon dioxide capture by chilled ammonia need to be addressed.

1.2 Research Objectives

The main research objective of this thesis work is to understand the effects of sulfur dioxide on the mass transfer of carbon dioxide into aqueous chilled ammonia. To achieve this goal, the following tasks were completed.

- Experimental studies of the effects of sulfur dioxide on mass transfer of carbon dioxide absorbed by chilled ammonia.
- Mathematical modeling of the effects of sulfur dioxide on carbon dioxide absorption by chilled ammonia

Finally, a general equation is proposed to quantify the effects of sulfur dioxide on mass transfer of carbon dioxide into chilled ammonia.

1.3 Thesis Structure

This thesis includes literature review, experimental section, mechanism, calculation, and modeling of simultaneous absorption of CO_2 and SO_2 with ammonia.

In the first chapter, literature review, existing abatement technologies are reviewed through a comparative study of different carbon dioxide absorbents. Then the mechanism of absorption of carbon dioxide into aqueous ammonia was investigated systematically.

In the third chapter, experimental setup, absorbent preparation, and experimental procedures are described in details.

In the fourth chapter, the mathematical model was developed. The reaction mechanism and mass transfer model were introduced in this chapter. Of particular importance is the calculation of the mass transfer coefficient of carbon dioxide absorbed by chilled ammonia.

The fifth chapter presents the modeling of carbon dioxide absorption by ammonia in the presence of sulfur dioxide. Reaction and mass transfer models for the specific situation for carbon dioxide and sulfur dioxide absorbed simultaneously by aqueous ammonia was investigated. Both analytical and numerical solutions were considered. Finally, based on the simulation results, a general equation was proposed to predict the effects of sulfur dioxide on mass transfer of carbon dioxide into ammonia.

Chapter 2 Literature Review

2.1 Carbon Dioxide Capture Technologies

Although many research projects have been conducted related to carbon capture from flue gas, the costs of installation and operation are still high comparing to those without carbon capture processes[8]. It was reported that 70%-80% of the total cost of carbon capture is for the transport and storage system[9]. There are three primary technologies associated with the different combustion system, pre-combustion, oxy-combustion, and post-combustion carbon capture.

2.1.1 Pre-combustion Carbon Capture

In pre-combustion carbon capture, fossil fuels are gasified into hydrogen and carbon monoxide. CO is then converted into hydrogen and CO_2 by the water-gas shift reaction, followed by CO_2 capture, typically using physical adsorption-based processes.

Partial oxidation is one of the primary reactions that converts solid fuels, like coal, to gaseous fuels through a fuel rich combustion process described in equation (R 2-1). This process converts most solid fuels to the products containing CO and H_2. Because of the relatively low temperature of partial oxidation, it minimizes the formation of NO_x, and the gaseous products are mainly CO and H_2, which is called syngas.

The chemical reaction of gasification process can be described as:

$$C_\alpha H_\beta + \frac{1}{\phi}\left(\alpha + \frac{\beta}{4}\right) O_2 \rightarrow [xCO_2 + (1-x)CO] + [yH_2O + (1-y)H_2] + zO_2 \qquad \text{(R 2-1)}$$

The syngas can be directly burned for energy production where CO is converted into CO_2 by oxidation. However, water–gas shift (WGS) is necessary to CO_2 capture, where the CO produced from partial oxidation is converted into CO_2, according to reaction (R 2-2):

$$CO + H_2O \rightarrow H_2 + CO_2 \qquad \text{(R 2-2)}$$

2.1.2 Oxy-combustion Carbon Capture

In oxyfuel combustion, oxygen instead of air is used as an oxidant. Such a process simplifies the subsequent separation of nitrogen molecules. Another advantage is a reduction of NOx in flue gas[10]. Because of the absence of nitrogen molecules in combustion, the major products of combustion are particulate matters, water, carbon dioxide and sulfur dioxide, if any.

Conventional electrostatic precipitator and FGD process could remove particulates and SO_2, respectively. The main drawback of this process is the large energy consumption associated with producing oxygen, resulting in an energy penalty of 7% compared with plants without oxyfuel combustion process[11]. Because of high SO_2 concentration in the flue gas, corrosion is another problem. At present, the implement of full-scale oxyfuel-fired power plants is still under research and development.

2.1.3 Post-combustion Carbon Capture

Post-combustion is a CO_2 capture process for the power plants and industrial facilities. This process captures the post-combustion carbon dioxide, which is much different from pre-combustion and oxyfuel combustion because of a more complex mix of components in the post-combustion products.

A typical flue gas contains 7-15% carbon dioxide, which is low for carbon dioxide capture by physical sorption[12]. The physical absorption is not as efficient as chemical absorption at such low CO_2 concentrations. Thus, chemical absorption is the most suitable technology in this case. The disadvantage caused by the low partial pressure of carbon dioxide in post-combustion process is compensated by its low cost for retrofitting the facilities.

However, since the CO_2 partial pressure in post-combustion flue gas is low (7-15%), the major barrier is large parasitic load resulting in energy penalty and associated costs. The energy cost to concentrate carbon dioxide (above 95.5%) is a major challenge. A 32% to 65% increasing of electricity cost caused by post-combustion carbon capture was reported[13].

2.1.4 Absorption

2.1.4.1 Physical absorption

Physical absorption is a process using a solvent to absorb separate a gas from the carrier gas. Henry's law can describe the absorption process. Physical absorption is usually used for high carbon dioxide partial pressure gas which has a larger solubility for solvent than with low partial pressure gas.

2.1.4.2 Chemical absorption

The sorbents used in chemical absorption are usually liquid sorbents. Heating or depressurization can regenerate the liquid sorbents. Typically, amine-based sorbents, such as monoethanolamine(MEA) and diethanolamine (DEA)[14], are used. MEA was found to be the most effective for carbon capture[13]. Piperazine and other solvents have attracted attention recently[15]. Though piperazine is more costly than MEA, it reacts with carbon dioxide much faster. Piperazine, as carbon dioxide absorbent, is still under development. Degradation of MEA is a major challenge to this process. Other challenges like equipment corrosion and degradation product nitramines, which are harmful to human are in the count too.

Chilled ammonia process is an aqueous ammonia-based carbon capture technology. This process reduces the loss of sorbent by operating under low temperature to decrease the volatility of aqueous ammonia. Waste heat is used to regenerate the solvent and carbon dioxide. The major advantage of this process is low energy cost[7] (2GJ/ton for

desorber compared with 3.7GJ/ton for MEA). Another advantage is less degradation comparing with amine-based absorption.

2.1.5 Adsorption

Different from absorption processes, adsorption processes use sorbent to adsorb carbon dioxide. The absorption efficiency is affected by interfacial surface area, selectivity and regeneration property. Activated carbon, zeolites, Rectisol, Selexol and calcium oxides are typical sorbents. The regeneration of carbon dioxide is much simpler than for absorption.

Pressure swing adsorption (PSA) or temperature swing adsorption (TSA) can be employed to recover carbon dioxide. It was reported that PSA used in a power plant can achieve a carbon dioxide recovery efficiency of above 85%[16]. Carbon dioxide will adsorb on the sorbent with high pressure and desorb with low pressure. For TSA, carbon dioxide is adsorbed with low temperature and desorbed with high temperature. TSA usually takes a longer time to recover carbon dioxide than PSA. However, the purity of regenerated carbon dioxide (95%) is relatively higher than in the PSA process (80%). The cost of operating TSA was around 80-150 US dollars per ton carbon dioxide captured[17].

2.1.6 Chemical Looping Combustion

During chemical looping combustion, a metal oxide instead of pure oxygen participates in the chemical reactions. This process consists of two reactors: one reactor where air oxidizes the reduced metal, and another reactor where the metal oxide reacts with the fuel to produce CO_2 and H_2O, as well as reduced metal, the latter being sent back to the first reactor. Those two reactors are typically interconnected fluidized bed reactors. The advantage of chemical looping combustion is the ease of separating carbon dioxide from water.

The metal oxides have many variants. Metal oxides suitable for carbon capture include Fe_2O_3, NiO, CuO, and Mn_2O_3. Inert support materials can increase the performance. However, the inert material should be considered together with metal oxide type[18]. The quickly decreasing oxidation reaction rate due to the formation of the unreactive iron compound with increasing number of cycles is the main drawback of this technology[19].

2.1.7 Hydrate-based Separation

Hydrate-based CO_2 separation technology can also separate CO_2 from flue gases.. The CO_2 in a flue gas will combine preferentially with hydrate cages to be separated from other gases. One advantage of this technology is the low energy consumption (0.57kWh/kg CO_2 comparing with 2.32kWh/kg CO_2 for using ammine[20]). To increase CO_2 capture efficiency decreasing the hydrate pressure is the alternative methods. One typical solvent for this technology is tetrahydrofuran (THF), which is water-miscible. THF is usually used as a thermodynamic promoter because it can form hydrate combination with water under a low temperature. The disadvantage of this technology is the requirement of high pressure during the formation of hydrate. From the economic point of view, the lower the pressure leads to lower the cost. Thus, this technology has not been commercialized[21].

Englezos et al.[22] reported that THF decreases the hydrate formation pressure and thus, the pressure required for CO_2 capture is decreased too, which reduces the energy penalty. The effects and mechanisms of the additive mixture on the hydrate phase equilibrium using the isochoric method have confirmed the effects of THF on hydrate formation. The hydrate base CO_2 separation technology is considered as one of the most promising CO_2 separation technology in the long-term[23].

2.1.8 Amine-based and Ammonia-based Chemical Absorption

Typical chemical absorption sorbents are carbonate-based, aqueous ammonia-based, hydroxide based and amine-based sorbents. One of the most mature technologies is amine-based CO_2 absorption but, as mentioned previously, this technology requires a large amount heat.

One alternative to amine-based solvents is aqueous ammonia. There are two main variants of this technology, depending on the operating temperature. When operated at low temperatures (0-20°C) the process is called chilled ammonia process. The main advantage of the low-temperature process is the reduced volatility of ammonia, and a reduced gas volume. Thus, the cost of ammonia supplement and utility will drop. In the chilled ammonia process (0-10°C), the precipitation of carbamate compound will form. Another variant of the process is when operating in the temperature range of 20-40°C.

Based on equilibrium calculations, Victor Darde[7] showed that the chilled ammonia process allows for a significant reduction in energy consumption in the regeneration step compared to the energy consumption of the process using amines.

2.2 Aqueous Ammonia-Based Chemical Absorption

Ammonia-based chemical absorption can absorb not only CO_2 but also other components in flue gases like SO_2 and NO_2. A by-product of this technology is ammonium salts, which can be used as a fertilizer. In a typical ammonia-based CO_2 capture process, the flow of ammonia will contact with flue gas in a counter-flow fashion. The temperature of operation is as low as 0-20°C, and thus the flue gas must be cooled before entering the absorber. The low temperature not only allows high absorption capacity of ammonia but also decreases the amount of ammonia being volatilized. The downstream gas enters a water washer to absorb residues ammonia to reduce ammonia slip. The CO_2 will be regenerated with a temperature around 90°C. To avoid ammonia volatilization, cold washer is also used in the regeneration process[2].

A well-accepted overall reaction for CO_2 capture by aqueous ammonia can be described as:

$$NH_3 + CO_2 + H_2O \rightarrow NH_4HCO_3 \qquad \text{(R 2-3)}$$

2.3 Knowledge Gap

Like amine, aqueous ammonia is a liquid chemical sorbent, but aqueous ammonia technology has two key advantages. First, aqueous ammonia is less expensive than amines ($0.66/kg CO_2 carrying capacity versus $8.4/kg. CO_2), which lowers the chemical make-up costs[24]. Second, aqueous ammonia has a lower heat of reaction (613 kJ/kg) for regenerating the chemical sorbent (compared to 1934 kJ/kg for mono-ethanol amine). For a typical coal-fired power plant of 300MW using coal with 1.2% sulfur content, the flue gas stream contains about 300 ppm SO_2 after wet desulfurization.[6] The effect of the presence of SO_2 for chilled ammonia CO_2 capture has not been well reported in literature It is important to understand the effects of SO_2 (6–300 ppm after wet desulfurization) on the performance of the CO_2 absorption with aqueous ammonia absorbent.

The mass transfer and kinetics of combined CO_2 and SO_2 absorption in aqueous NH_3 were investigated at various SO_2 concentrations, temperatures and aqueous NH_3 concentrations in a wetted wall column by Qi et al.[25]. The SO_2 absorption in the SO_2 instantaneous reaction region is considered to form a thin film with low active NH_3 and high produced sulfite levels, which reduce the efficiency and kinetics of CO_2 absorption. Their study was carried out at temperatures between 20 and 80°C, and thus not applicable for the chilled ammonia process.

A. Effect of mass transfer coefficient of carbon dioxide absorbed by ammonia

The sulfur dioxide downstream of a FGD process may have an effect on the carbon dioxide mass transfer when absorbed by aqueous ammonia. To quantify the effect of

sulfur dioxide on CO_2 absorption, the study of volumetric liquid-phase mass transfer is necessary. Mass transfer coefficient varies with liquid-gas reactor, liquid load, and solvent concentration.

B. The general method that can be used to estimate the sulfur dioxide effect on carbon dioxide mass transfer when absorbed by aqueous ammonia

When simplifying the method to estimate the SO_2 effects for the real-life problem, a mathematical model is needed for the ease of use. Further, a more general equation can be obtained by summarizing the mathematical model. The general equation will be a convenient method to predict the sulfur dioxide effect of carbon dioxide absorption by ammonia in flue gas treatment process.

Chapter 3 Experimental Section and Determination of Mass Transfer Coefficient

3.1 Introduction

Before estimating the effects of SO_2 on mass transfer coefficient of carbon dioxide absorption by aqueous ammonia, it is necessary to study the mass transfer coefficient of carbon dioxide in aqueous ammonia. Similar experiments have been conducted by Qin et al.[26] They used wetted falling wall reactor and determined the mass transfer coefficient of carbon dioxide absorbed by aqueous ammonia in a temperature range (20- 80°C). However, the low temperature (0-10°C) data is missing which is essential for chilled ammonia process.

In this work, the experiments were carried out with a double stirring tank reactor as shown in Figure 3-1. The experimental set up for determining mass transfer coefficients of CO_2 in aqueous ammonia, with or without the presence of SO_2, is shown in Figure 3-1. The inlet gas from cylinders was mixed in the gas mixer. The flow rate of the stream from each cylinder was adjusted to obtain desired concentrations of the gas mixture (composed of N_2, CO_2 and SO_2). Mass flow controllers (0-10SLPM, Cole-Parmer) were used to control and monitor the gas flow rates. A gas mixer (1-800-STATICS, Koflo) was used to ensure the gases mixed well. The simulated flue gas could include SO_2 for concentrations ranging from 0 to 4000 ppm and fed at 2 L/min. A three-way valve that could be switched between bypass and gas feed was placed downstream from the mixer.

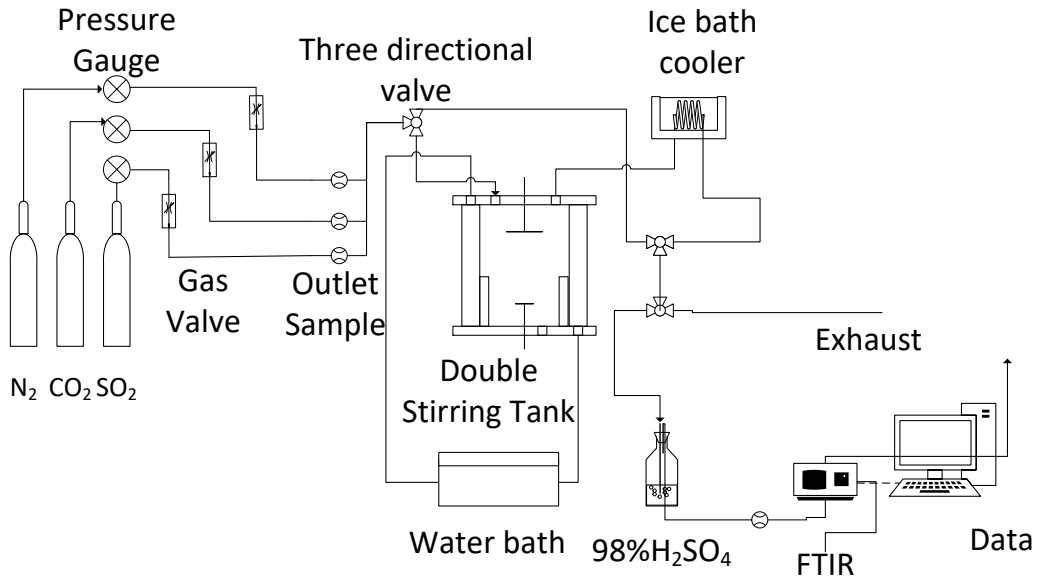

Figure 3-1. Experimental setup for the determination of mass transfer coefficient of CO_2 in aqueous ammonia

The gas stream was fed to the double stirring tank trough the opening in the top of the double stirring tank. 500 ml of aqueous ammonia of desired concentration (and verified through titration method) was prepared. The pH values of the liquids were measured using a benchtop pH meter with an accuracy of ±0.01 (Model pH700 from Oakton Instruments). The prepared solution was then transferred to the customized double-stirred tank reactor, as illustrated in Figure 3-2. The stainless steel reactor was a vessel with an inner diameter of 99.7 mm and an outer water jacket with an inner diameter of 152.4 mm for temperature control. Four rectangular baffles that were 9.5 mm wide ensured a flat

surface during stirring. Both stirrers were paddle-type impellers. The gas-phase stirrer was a four-bladed impeller with straight, flat blades and a diameter of 54.0 mm, and the liquid-phase stirrer was an eight-bladed impeller with straight, flat blades and a diameter of 38.1 mm. The top and bottom shafts were driven by two mixers (Model RK-50705-00 from IKA Works, Inc.). The speed of the mixer was set at 700 rpm for gas phase and 230 rpm for the liquid phase. Two love-joy couplings were used to control vibration. The absorber was operated continuously about the gas phase and batch-wise with the liquid phase. The outlet gas from the double stirring tank was cooled through ice bath to remove the water vapor. If a significant amount of water vapor transferred to the Fourier transform infrared spectrometer (FTIR, MKS Instruments MultiGas Model 2030), it would not only affect the measuring accuracy but also could dirty the mirror in a gas cell in FTIR. As such, a concentrated sulfuric acid wash bottle containing 200 ml of 98% sulfuric acid was used as the reactor outlet gas before going to the FTIR.

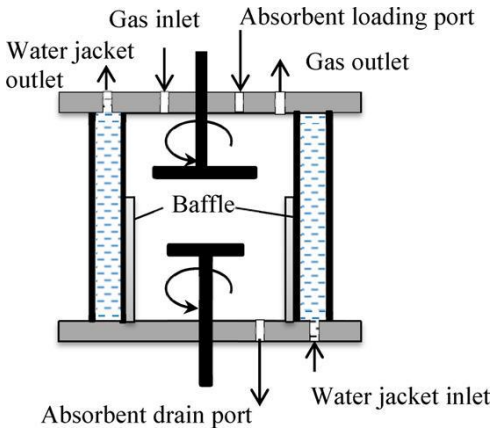

Figure 3-2 Diagram of double stirring tank

In a typical run, gas concentration from the reaction was continuously monitored by the FTIR. Once a stable concentraiton of carbon dioxide concentration is recorded for a

period of time, the experiment was completed. The concentrations of ammonia water were titrated after the experiment.

3.2 Validation of Simulated Flue Gas

By using a mixing gas system, the accuracy of the concentration of the synthesized gas needs to be ensured, which was realized by analyzing the mixed gases using the FTIR. Desired carbon dioxide concentrations are between 2% to 15%, and desired concentrations of sulfur dioxide are between 0 and 4000 ppm. Table 3-1shows the calculating and reading values of gas concentrations. The cylinders of CO_2 and SO_2 used in this validation are 15% and 1%, except for the 3000 and 4000 ppm SO_2. For those high concentrations of SO_2, cylinders with 50% CO_2 and 10% SO_2 were used. The agreement between desired and measured values was less than 5%. Preliminary experiments show that a 10% variation in concentration of inlet carbon dioxide will have a slight effect (1%-5%) on the record of the concentration of carbon dioxide in the outlet stream.

Table 3-1 Comparison between desired SO_2 and CO_2 concentrations of the simulated flue gas with the actual concentrations as measured by FTIR.

Number	SO_2 (ml/min)	CO_2 (ml/min)	N_2 (ml/min)	Calculated SO_2 (ppm)	Calculated CO_2	Measured SO_2 (ppm)	Measured CO_2
1	0	133	1866	0	1%	0	0.93%
2	0	266	1766	0	2%	0	2.11%
3	0	400	1600	0	3%	0	3.09%
4	0	533	1466	0	4%	0	4.10%

5	100	266	1633	500	2%	511	2.09%
6	200	266	1533	1000	2%	1049	2.10%
7	300	266	1433	1500	2%	1540	2.13%
8	400	266	1333	2000	2%	1960	2.12%
9	60	80	1860	3000	2%	2981	2.11%
10	80	80	1840	4000	2%	4034	2.08%

3.3 An Example of FTIR Data

An example of FTIR data is shown in Figure 3-3. The line in the graph indicates the change of concentration of carbon dioxide from the reactor outlet. The desired concentration of carbon dioxide was set before the gas is fed to the reactor (In the case of Figure 3-3, the desired concentration of carbon dioxide is 2%). After a stable concentration of carbon dioxide in the feed gas had been monitored (while bypassing the reactor), the gas was fed to the reactor. In Figure 3-3, the sharp decrease of concentration of carbon dioxide indicates the time when the feed gas mixture was directed to the reactor and was absorbed by ammonia. In this particular case, the reaction in the reactor reached steady state in about 60 seconds. The concentration of carbon dioxide in the outlet gas was calculated using average outlet concentration after reaching steady state.

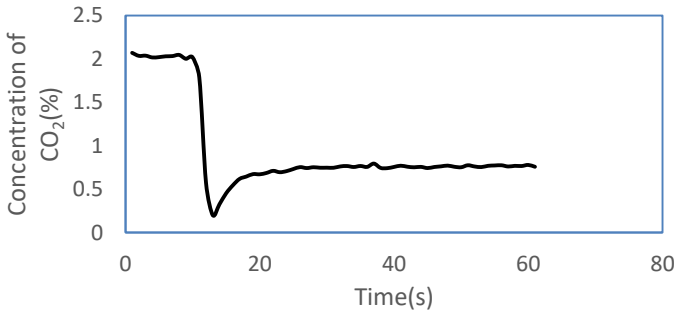

Figure 3-3 An example of FTIR data

3.4 Mass Transfer of CO_2 into Aqueous Ammonia

The mass transfer process with gas-liquid chemical absorption can be explained based on the two-film theory discussed in section 4.1. The rate of CO_2 absorption into ammonia can be expressed, based on mass balance and the ideal gas law, as follows:

$$P_{CO_2}V = n_{CO_2}RT \qquad (3\text{-}1)$$

where P_{CO_2} is partial pressure of carbon dioxide, Pa

V is volume of gas, L

n_{CO_2} is mass amount of carbon dioxide, mol

R is ideal gas constant, Pa L mol^{-1} K^{-1}

T is gas temperature, K

The reaction during absorption of carbon dioxide in aqueous ammonia is typically second order[25]. In the case of the second order reactions, the determination of the enhancement factor can be rather complex. However, it is possible to apply conditions where the concentrations of the reactants are constant in the solution, which implies that the reactant ammonia is not considerably depleted at the gas-liquid interface. Under these conditions,

from the double film theory, the expression of the enhancement factor has been reported that the rate of CO_2 absorption into ammonia can be calculated by the mass difference of inlet and outlet of CO_2[27]. The derivation of enhancement factor will be discussed in section 5.3.

Based on the mass balance, the amount of carbon dioxide inducted to the reactor should be equal to the sum of the amount of carbon dioxide absorbed by absorbent and in the outlet stream. Thus, the mass balance can be expressed as follows:

$$\left\{\begin{array}{c} Flux\ of \\ carbon\ dioxide \\ absorbed\ into \\ aqueous\ ammonia \end{array}\right\} = \left\{\begin{array}{c} Flux\ of \\ carbon\ dioxide \\ in\ inlet\ stream \end{array}\right\} - \left\{\begin{array}{c} Flux\ of \\ carbon\ dioxide \\ in\ outlet\ stream \end{array}\right\} \quad (3\text{-}2)$$

The molar flux of CO_2, N_{CO_2}, is the number of moles per unit time per unit area, generally:

$$N_{CO_2} = \frac{n}{St} \quad (3\text{-}3)$$

Where: S is area of surface of liquid phase, m^2

t is time of n mol carbon dioxide to through the surface, s

The number of moles of carbon dioxide can be calculated by equation (3-1):

$$n = \frac{P_{CO_2}V}{RT} \quad (3\text{-}4)$$

The ratio of volume and time is known as volume flow rate Q which can be monitored by flow meter during experiment:

$$Q = \frac{V}{t} \quad (3\text{-}5)$$

Substitute equations (3-4) and (3-5) to (3-3):

$$N_{CO_2} = \frac{Q}{RTS} P_{CO_2} \tag{3-6}$$

The flux of carbon dioxide in the reactor inlet stream,$N_{CO_2,in}$, can thus be determined knowing the inlet volume flow rate, Q_{in}, and the partial pressure of carbon dioxide in inlet stream of the reactor, $P_{CO_2,in}$, which are determined from the experimental data.

Substitute $N_{CO_2,in}$, Q_{in} and $P_{CO_2,in}$ into Eq. (3-5) and the flux of carbon dioxide in inlet stream can be determined as:

$$N_{CO_2,in} = \frac{Q_{in}}{RTS} P_{CO_2,in} \tag{3-7}$$

Similarly, the molar flux of carbon dioxide in the reactor outlet stream, $N_{CO_2,out}$, can be determined, using Eq. (3-8):

$$N_{CO_2,out} = \frac{Q_{out}}{RTS} P_{CO_2,out} \tag{3-8}$$

The molar flux of carbon dioxide absorbed into aqueous ammonia (See Eq. 3-2) can be rewritten as:

$$N_{CO_2} = N_{CO_2,in} - N_{CO_2,out} \tag{3-9}$$

or

$$N_{CO_2} = \frac{Q_{in}}{RTS} P_{CO_2,in} - \frac{Q_{out}}{RTS} P_{CO_2,out} \tag{3-10}$$

The volumetric flow rate change caused by absorption of carbon dioxide and sulfur dioxide by ammonia is considered negligible because of the low concentrations of carbon

dioxide (2%) and sulfur dioxide (ppm level). Thus, the volumetric flow rate of inlet and outlet streams of reactor can be assumed the same:

$$Q_{in} = Q_{out} \tag{3-11}$$

Then, Eq. (3-10) becomes

$$N_{CO_2} = \frac{Q_{in}}{RTS}(P_{CO_2,in} - P_{CO_2,out}) \tag{3-12}$$

where N_{CO_2} is mass transfer flux of carbon dioxide absorbed by aqueous ammonia, mol cm^{-2} s^{-1}

$P_{CO_2,in}$is partial press of carbon dioxide in the inlet stream of reactor, Pa

$P_{CO_2,out}$is partial pressure of carbon dioxide in the outlet stream of reactor, Pa

Q_{CO_2} is volumetric flow rate of inlet gas, L s^{-1}

The experimental results of N_{CO_2} calculated using equation (3-12) will be used to fit and validate the model.

The value of N_{CO_2} from experiment will be used to calculate the overall CO_2 gas-phase mass transfer coefficient, K_G, which will be discussed in Chapter 4. The determined N_{CO_2} by experiment will be used to determine K_G as shown in Equation (3-13):

$$K_G = -\frac{N_{CO_2}}{P_{gb} - P_{gb}^*} \tag{3-13}$$

where

P_{gb} is log mean average of gas bulk CO_2 partial pressure, Pa.

P_{gb}^{*} is gas-phase CO_2 concentration that would be in equilibrium with the bulk liquid concentration, Pa. In this work in bulk aqueous ammonia concentration was assumed to be 0.

The log mean average of operational gas bulk CO_2 partial pressure P_{gb} can be calculated using Eq. 3-14[28]:

$$P_{gb} = \frac{P_{CO_2,in} - P_{CO_2,out}}{Ln(P_{CO_2-in}/P_{CO_2-out})} \tag{3-14}$$

The mass transfer coefficient of carbon dioxide can be written as equation (3-15):

$$K_G = \frac{Ek_L}{H_c} \tag{3-15}$$

The derivation of Eq. (3-15) and the explanation of enhancement factor E will be introduced in section 5.3

Substitute Eqs. (3-13) to (3-17) to have:

$$N_{CO_2} = \frac{Ek_L}{H_c}(P_{gb} - P_{gb}^{*}) \tag{3-16}$$

To find the enhancement factor E in equation (3-16), a dimensionless parameter Hatta number Ha that compares the rate of reaction in a liquid film to the rate of diffusion through the film can be used and is defined as[29]:

$$Ha = \frac{\sqrt{k_f D_c}}{k_L} \tag{3-17}$$

For the absorption of carbon dioxide into aqueous ammonia, the reaction is a pseudo-first-order reaction. The above model can be applied. The pseudo-first-order reaction rate with respect to carbon dioxide is shown in equation (4-44). The derivation of Hatta number in this work is discussed in section 5.3 from Eqs. (5-16) to (5-25).

$$Ha = \frac{\sqrt{k_{obs} D_{CO_2-NH_3}}}{k_L} \tag{3-18}$$

The molar flux of carbon dioxide absorbed in liquid phase N_{CO_2} is derived in section 5.3, equation (5-23) to (5-37) and gives:

$$N_{CO_2} = C_0 k_L Ha \tanh Ha \tag{3-19}$$

The term $Ha \tanh Ha$ is the enhancement factor$E$:

$$E = Ha \tanh Ha \tag{3-20}$$

Hyperbolic tangent can be derived as:

$$\tanh Ha = \frac{\sinh Ha}{\cosh Ha} = \frac{e^{Ha} + e^{-Ha}}{e^{Ha} - e^{-Ha}} = \frac{e^{2Ha} + 1}{e^{2Ha} - 1} = \frac{1 - e^{-2Ha}}{1 + e^{-2Ha}} \tag{3-21}$$

For pseudo-first-order reactions, the Hatta number is much larger than 1, and thus the term e^{-2Ha}in equation (3-21) is negligible. Thus:

$$\tanh Ha \approx 1 \tag{3-22}$$

and so,

$$E = H \tag{3-23}$$

Substituting equations (3-18) and (3-23) to (3-16), it comes:

$$k_{obs} = \frac{N_{CO_2}^2 H_c^2}{P_{gb} D_{CO_2-NH_3}} \tag{3-24}$$

The value of k_{obs} can be determined by substituting N_{CO_2} in equation (3-24) . N_{CO_2} is calculated using equation (3-12) from experimental data. P_{gb} is calculated by equation (3-14). The methods for calculating H_c and $D_{CO_2-NH_3}$ are shown in section 0. Then, the value of k_{obs} determined from experimental data can be used to determine Hatta number in equation (3-18). Thus, the value of enhancement factor E is calculated using (3-23). The k_{obs} is representing the reaction rate between carbon dioxide and ammonia which derivation will be given in section 4.3 from equation (4-47) to (4-51). The value of k_{obs} will be used to calculated the pseudo-first-order reaction rate k_{f1} shown in section 4.3 in equation (4-51) and (4-52).

Chapter 4 Model Development and Calculations

The mass transfer rate of CO_2 and SO_2 from the gas phase to aqueous NH_3 can be described by the two film model with pseudo-first-order reaction with respect to CO_2. Caplow[30] and Derks and Versteeg[31] reported that the CO_2 mass transfer in aqueous NH_3 is similar to that in the primary amine, which can be explained according to a pseudo-first-order reaction mechanism. Based on the two-film theory, the NH_3 concentration in the liquid film is expected to be little different from that in the bulk liquid, and there is little diffusion limitation when the reaction between CO_2 and NH_3 occurs.

Correspondingly, Qin et al.[26] reported that the CO_2 mass transfer process in aqueous NH_3 is determined by the reaction rate, and explained this using a pseudo-first-order reaction mechanism by diffusion limitation and reaction rate between CO_2 and NH_3. The reaction kinetics of ammonia and SO_2 was studied by Hikita[32] which can be considered as an instantaneous reaction.

The absorption of CO_2 into an ammonia solution is a complex process that generates different products at various CO_2 loadings and temperatures[7]. The most well known mechanism to explain the reaction between primary amine and CO_2 is the zwitterion mechanism, which is described in details in the next section.

4.1 Two Film Theory

In this theory, film transport is governed essentially by molecular diffusion. Therefore, Fick's law describes flux through the film.

$$J = -D\frac{\partial C}{\partial X} \tag{4-1}$$

Where:

J is flux of C through the film.

X is length in direction the flux through

C is the concentration of carbon dioxide.

D is the diffusion coefficient of carbon dioxide in liquid phase

If the thickness of the stagnant film is given by δ then the gradient can be approximated by

$$\frac{\partial C}{\partial X} \approx \frac{C_b - C_i}{0 - \delta} \tag{4-2}$$

Where:

$C_b$is concentration in bulk

$C_i$is concentration at interface.

δ is thickness of stagnant film.

At steady state if there are no reactions in the stagnant film there will be no accumulation in the film (Assume that D is constant) therefore the gradient must be linear and the approximation is appropriate.

$$J = -D\frac{C_b - C_i}{0 - \delta} \tag{4-3}$$

To simplify calculations a mass transfer coefficient is usually defined for either the liquid or gas phase as k_L or k_G[28].

$$k_L = \frac{D_L}{\delta_L} \tag{4-4}$$

Where $D_L \; and \delta_L$ are diffusion coefficient and film thickness for liquid phase, respectively.

k_L is liquid-phase mass transfer coefficient s^{-1}

k_G gas-phase mass transfer coefficient mol s^{-1} m^{-2} atm^{-1}

In the case of gas-liquid transfer, we have transfer considerations from both sides of the interface. We use the Lewis-Whitman[33] two-film model as described below in Figure 4-1.

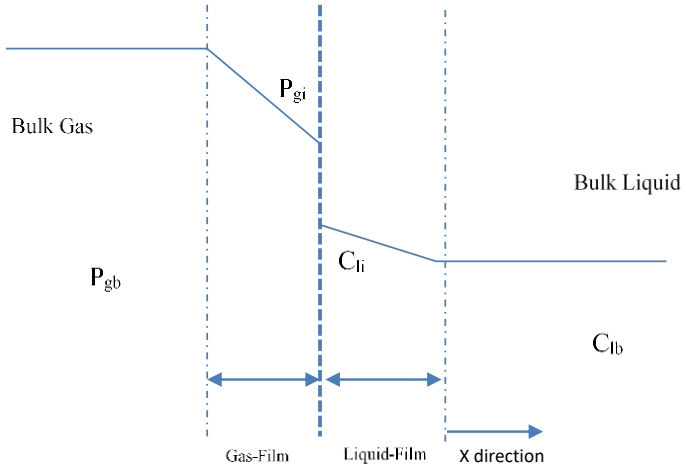

Figure 4-1 The diagram of two-film model

We can assume that equilibrium is attained at the interface

$$C_{li} = \frac{P_{gi}}{H_c} \tag{4-5}$$

Where:

H_c is Henry's constant for carbon dioxide, L pa mol^{-1}

C_{li} is equilibrium concentration of carbon dioxide in liquid interface, mol L^{-1}

P_{gi} is partial pressure of carbon dioxide in gas interface, pa

A steady-state flux balance through each film can now be performed. The fluxes are given by:

$$\mathrm{J} = k_L(C_{lb} - C_{li}) \tag{4-6}$$

$$\mathrm{J} = k_G(P_{gi} - P_{gb}) \tag{4-7}$$

P_{gb} is partial pressure of carbon dioxide in gas bulk, pa

If a reaction of transferred gas is taking place in the liquid phase, the enhancement factor E is applied. E is the so-called enhancement factor (dimensionless) which is the ratio of the absorption rate with and without the reaction for the same concentration difference. The flux of liquid phase can be rewritten as:

$$\mathrm{J} = Ek_L(C_{lb} - C_{li}) \tag{4-8}$$

Concentrations at the interface cannot be measured. Thus, overall mass transfer coefficients are defined. These coefficients are based on the difference between the bulk

concentration in one phase and the concentration that would be in equilibrium with the bulk concentration in the other phase.

Define:

$$\mathrm{J} = K_L(C_{lb} - C_{lb}^*) \tag{4-9}$$

$$\mathrm{J} = K_G(P_{gb}^* - P_{gb}) \tag{4-10}$$

$$C_{lb}^* = \frac{P_{gb}}{H_c} \tag{4-11}$$

$$P_{gb}^* = C_{lb}H_c \tag{4-12}$$

K_L is overall mass transfer coefficient based on liquid-phase concentration

K_G is overall mass transfer coefficient based on gas-phase concentration.

C_{lb}^* is liquid-phase concentration that would be in equilibrium with the bulk gas concentration

$P_{gb}^*$is gas-phase concentration that would be in equilibrium with the bulk liquid concentration

Expand the liquid-phase overall flux equation to include the interface liquid concentration.

$$\mathrm{J} = K_L([C_{lb} - C_{li}] + [C_{li} - C_{lb}^*]) \tag{4-13}$$

Then substitute

$$C_{li} = \frac{P_{gi}}{H_c} \; and \; C_{lb}^{*} = \frac{P_{gb}}{H_c} \tag{4-14}$$

into equation (4-13) leading to:

$$\mathrm{J} = K_L\left([C_{lb} - C_{li}] + [P_{gi} - P_{gb}]/H_c\right) \tag{4-15}$$

In the steady state, fluxes through all films must be equal. Let all these fluxes be equal to J. On an individual film basis:

From eq (4-8): $$\frac{J}{Ek_L} = (C_{lb} - C_{li}) \tag{4-16}$$

From eq (4-7): $$\frac{J}{k_G} = (P_{gi} - P_{gb}) \tag{4-17}$$

Then equation (4-15) becomes:

$$\mathrm{J} = K_L\left(\frac{J}{Ek_L} + \frac{J}{k_G H_c}\right) \tag{4-18}$$

Since all J's are equal, equation (4-18) can be arranged to give:

$$\frac{1}{K_L} = \frac{1}{Ek_L} + \frac{1}{k_G H_c} \tag{4-19}$$

A similar manipulation starting with the overall flux equation based on gas-phase concentration will give:

$$\frac{1}{K_G} = \frac{H_c}{Ek_L} + \frac{1}{k_G} \tag{4-20}$$

Equations (4-19) and (4-20) can be viewed as "resistance" expressions where $\frac{1}{K_G}$ or $\frac{1}{EK_L}$ represent total resistance to mass transfer based on gas or liquid-phase concentration, respectively.

The mass transfer can be expressed in terms of driving potential and the corresponding resistance;

$$\frac{C_{lb} - C_{lb}^*}{R} = \frac{C_{lb} - C_{lb}^*}{R_L + R_G} \tag{4-21}$$

$$R = R_L + R_G$$

Where R, R_L and R_G are overall resistance, liquid-phase resistance, and gas-phase resistance to mass transfer, respectively.

$$R = \frac{1}{K_G}, R_L = \frac{H_c}{Ek_L}, R_G = \frac{1}{k_G} \tag{4-22}$$

Because of the low solubility of carbon dioxide in water, Henry's law constant is high. The term $\frac{H_c}{Ek_L}$ has high value. Then, the mass transfer resistance is primarily attributed to the liquid phase. The gas-phase mass transfer resistance is negligible:

$$R \approx R_L \tag{4-23}$$

That is

$$\frac{1}{K_G} = \frac{H_c}{Ek_L} \tag{4-24}$$

Which gives

$$K_G = \frac{Ek_L}{H_c} \tag{4-25}$$

Equation (4-25) will be used to calculate enhancement factor by determining K_G from experimental data, as shown in Appendix C- Experimental data. However, in this thesis work, the value of enhancement factor E in the numerical calculation with Matlab code was calculated but not presented in the result section. The molar flux of carbon dioxide is used rather than enhancement factor in result presenting part.; Interested readers can use the data to calculate the value of E.

4.2 Zwitterion Mechanism

Proposed by Caplow[30], the zwitterion mechanism shows the zwitterion will be formed by CO_2 and NH_3 first (R 4-1)followed by deprotonation through transfer of proton to base (B) in solution (e.g. NH_3 or H_2O) (R 4-2)

$$CO_2 + NH_3 \underset{k_{b1}}{\overset{k_{f1}}{\rightleftharpoons}} NH_3^+COO^- \quad \text{(R 4-1)}$$

$$NH_3^+COO^- + B \xrightarrow{k_{f2}} NH_2COO^- + BH^+ \quad \text{(R 4-2)}$$

Because both of reaction(R 4-2) and reaction(R 4-1) are consuming carbon dioxide. The overall reaction rate for carbon dioxide is the sum of reaction(R 4-1) and (R 4-2)

The forward reaction rate r_+ for the formation of carbamate $NH_3^+COO^-$is:

$$r_1 = k_{f1}[NH_3][CO_2] \quad (4\text{-}26)$$

The reaction (R 4-2), proton transfer reaction, is fast and thus it can be assumed that the product of the reaction (R 4-1) is consumed instantaneously. Also, the concentration of carbamate is very low and thus, the breakdown reaction of carbamate to carbon dioxide and ammonia is negligible. Therefore, the breakdown reaction rate of carbamate r_- is determined from reaction (R 4-2):

$$r_2 = k_{f2}[NH_3^+COO^-][B] \quad (4\text{-}27)$$

Because of the low solubility of carbon dioxide in aqueous ammonia, the concentration of carbon dioxide is small. The reaction is pseudo-first-order reaction, which is a fast reaction. The reaction can be considered to have reached equilibrium in this study. The equilibrium of formation of carbamate reaction (R 4-1) is:

$$r_{forward} = r_{backward} \tag{4-28}$$

$$k_{f1}[NH_3][CO_2] = k_{b1}[NH_3^+COO^-] \tag{4-29}$$

$$\frac{[NH_3][CO_2]}{[NH_3^+COO^-]} = \frac{k_{b1}}{k_{f1}} \tag{4-30}$$

$$[NH_3^+COO^-] = \frac{[NH_3][CO_2]k_{f1}}{k_{b1}} \tag{4-31}$$

The reaction rate of carbamate formation (4-26) can be rewritten as:

$$\frac{r_1}{k_{f1}} = [NH_3][CO_2] \tag{4-32}$$

$$r_1 = \frac{[NH_3][CO_2]}{\frac{1}{k_{f1}}} \tag{4-33}$$

Substitute the equilibrium concentration of $[NH_3^+COO^-]$ in equation (4-31) to break down reaction rate (4-27):

$$r_2 = k_{f2}\frac{[NH_3][CO_2]k_{f1}}{k_{b1}}[B] \tag{4-34}$$

$$\frac{r_2 k_{b1}}{k_{f1} k_{f2}[B]} = [NH_3][CO_2] \tag{4-35}$$

$$r_2 = \frac{[NH_3][CO_2]}{\frac{k_{b1}}{k_{f1} k_{f2}[B]}} \tag{4-36}$$

Because the carbon dioxide is consumed by both reactions of (R 4-1) and (R 4-2) and produced different productions so the total reaction rate is sum of formation (4-33) and break down reaction rate (4-36):

$$r_{CO_2-NH_3} = r_1 + r_2 \tag{4-37}$$

$$r_1 + r_2 = \frac{[NH_3][CO_2]}{\frac{1}{k_{f1}}} + \frac{[NH_3][CO_2]}{\frac{k_{b1}}{k_{f1} k_{f2}[B]}} \tag{4-38}$$

$$= \frac{[CO_2][NH_3]}{\frac{1}{k_{f1}} + \frac{k_{b1}}{k_{f1}} \frac{1}{k_{f2}[B]}} \tag{4-39}$$

The overall reaction rate $r_{CO_2-NH_3}$ is then given by:

$$r_{CO_2-NH_3} = \frac{[CO_2][NH_3]}{\frac{1}{k_{f1}} + \frac{k_{b1}}{k_{f1}} \frac{1}{k_{f2}[B]}} \tag{4-40}$$

When CO_2 is absorbed in an unloaded NH_3 solution, reactions (R 4-3) and (R 4-4) will contribute to the overall absorption rate at high pH values[26]. The reaction with OH^- ions leads to the formation of bicarbonate (R 4-3) and the carbon dioxide reacts with free ammonia molecules generates carbamate (R 4-1). The production of carbonic acid by CO_2 and H_2O is very slow(R 4-4) compared with reactions (R 4-3) and (R 4-2), and therefore, is negligible[34].

$$CO_2 + OH^- \xrightarrow{k_{OH^-}} HCO_3^- \quad \text{(R 4-3)}$$

$$CO_2 + H_2O \xrightarrow{k_{H_2O}} HCO_3^- + H^+ \quad \text{(R 4-4)}$$

That is to say, all the ammonia carbamate zwitterion compounds generated in reaction (R 4-1) would be instantaneously consumed in reaction (R 4-2). Therefore, reaction (R 4-1) is the rate-determining step. The overall reaction was first order with respect to CO_2 and NH_3, respectively.

4.3 Chemical Absorption SO_2 by Aqueous Ammonia Mechanism

When the sulfur dioxide is absorbed in ammonia hydroxide, the following two-step reactions will take place in the liquid phase[35].

$$SO_2 + NH_3 + H_2O \rightleftharpoons NH_4^+ + HSO_3^- \quad \text{(R 4-5)}$$

$$HSO_3^- + NH_3 \rightleftharpoons NH_4^+ + SO_3^{2-} \quad \text{(R 4-6)}$$

Combining reactions (R 4-5) and (R 4-6) the overall reaction is:

$$SO_2 + 2NH_3 + H_2O \rightleftharpoons 2NH_4^+ + SO_3^{2-} \quad \text{(R 4-7)}$$

Both of reactions, (R 4-5)and (R 4-6) are very fast and the reaction (R 4-7) may be considered as an instantaneous reaction.

4.4 Correction of the Reaction Rate for Hydroxyl Ions

Aqueous ammonia is a weak alkali solution. The hydroxyl ions will react with dissolved carbon dioxide in ammonia solution. The effect of hydroxyl ions was suggested to be considered by Pinsent[36]. The reaction rate of carbon dioxide absorbed by aqueous ammonia is determined by reactions (R 4-3) and (R 4-1) as shown in equation (4-41):

$$r_{overall} = r_{CO_2-NH_3} + k_{OH^-}[OH^-][CO_2] + k_{H_2O}[H_2O][CO_2] \quad (4\text{-}41)$$

Where：

$r_{overall}$ is overall reaction rate for CO_2 absorption, mol $L^{-1}s^{-1}$

$r_{CO_2-NH_3}$ is reaction rate of (R 4-1) and (R 4-2) represented by equation (4-40), mol $L^{-1}s^{-1}$

The reaction rate constant of carbon dioxide an hydroxyl ions can be calculated by[36]:

$$\log(k_{OH^-}) = 11.13 - \frac{2530}{T} \quad (4\text{-}42)$$

Where: T is temperature K.

The reaction between carbon dioxide and water is slow compared with that of carbon dioxide reacting with ammonia and hydroxide ion. Therefore, the term of reaction between carbon dioxide and water is negligible. Equation (4-41) can be rewritten as:

$$r_{overall} = r_{CO_2-NH_3} + k_{OH^-}[OH^-][CO_2] \quad (4\text{-}43)$$

Because the reaction (R 4-2) is proton transfer reaction, the reaction rate constant k_{f2} is very large and the reactant B in this study, ammonia, is in excess, thus $k_{f2}[B] \gg \frac{k_{b1}}{k_{f1}}$ [36].

The term $\frac{k_{b1}}{k_{f1}}\frac{1}{k_{f2}[B]}$ in equation (4-40) is thus negligible and the equation (4-39) can be rewritten as:

$$r_{CO_2-NH_3} = \frac{[CO_2][NH_3]}{\frac{1}{k_{f1}}} \tag{4-44}$$

$$r_{CO_2-NH_3} = k_{f1}[CO_2][NH_3] \tag{4-45}$$

Substitute equation (4-45) to equation (4-43). The overall reaction rate of CO_2 absorption can be rewritten as:

$$r_{overall} = k_{f1}[NH_3][CO_2] + k_{OH^-}[OH^-][CO_2] \tag{4-46}$$

The overall reaction rate could be defined as:

$$r_{overall} = k_{obs}[CO_2] \tag{4-47}$$

Where k_{obs} is called the observed reaction rate constant with respect to CO_2, s^{-1}.

The observed reaction rate constant k_{obs} could be determined by

$$k_{obs} = \frac{r_{overall}}{[CO_2]} \tag{4-48}$$

$$k_{obs} = k_{f1}[NH_3] + k_{OH^-}[OH^-] \tag{4-49}$$

Where the first term in equation (4-49) is called apparent reaction rate, k_{app}:

$$k_{app} = k_{f1}[NH_3] \tag{4-50}$$

Furthermore, the apparent pseudo-first-order reaction rate constant k_{app} of the carbamate formation from NH_3 and CO_2 could be obtained by

$$k_{app} = k_{obs} - k_{OH^-}[OH^-] \quad (4\text{-}51)$$

Where: k_{app} is the apparent pseudo-first-order reaction rate constant of carbamate formation by NH_3 and CO_2 reaction, s^{-1}

The observed reaction rate constant with respect to carbon dioxide k_{obs} can be determined experimentally. The experimental data can be found in Appendix C-Experimental data. Details about the determination of k_{obs} from experimental data are given in section 3.4.

After, the apparent reaction constant k_{app} is determined by equation (4-51). Thus, the second order reaction rate constant k_{f1} of carbamate formation can then be calculated by

$$k_{f1} = \frac{k_{app}}{[NH_3]} \quad (4\text{-}52)$$

This equation will be used to determine the reaction constant of carbon dioxide and ammonia reaction in the numerical calculations in section 5.3. The results of k_{f1}determined experimentally in this work is similar to those in the work of Yu[37] who was using similar reactor and conditions, showing the reliability of the experimental data of this work.

Chapter 5 Modeling of Simultaneous Absorption of SO_2 and CO_2 in NH_3

5.1 Simultaneous Absorption of Two Gases in Ammonia

In this work, the presence of sulfur dioxide in carbon dioxide will cause both gases to absorb in aqueous ammonia. In the present case, as mentioned in the previous chapter, the absorption of SO_2 is considered instantaneous. Therefore, the case considered here is that of simultaneous absorption of two gases in reactive liquid, one gas reacting instantaneously with a reactive species in a liquid medium. Another common example of this situation is the absorption of a gas mixture of hydrogen sulfide and carbon dioxide in alkanol ammonia solutions, which is quite similar to the system of study here. Therefore, the method can be applied for this study. This problem has been analyzed with the film theory by Ramachandran[38].

Gas absorption reaction between dissolved gases A and B and liquid-phase regent C has been investigated by Hikita[39] and Goettler[40]. The problem of simultaneous absorption of two gases A and B into a liquid containing reactant C can be represented by the following reactions:

$$\mathrm{C} + \nu_A A \rightarrow products \qquad \text{(R 5-1)}$$

$$\mathrm{S} + \nu_B A \rightarrow products \qquad \text{(R 5-2)}$$

Where C, S and A are carbon dioxide, sulfur dioxide and aqueous ammonia in this study. Stoichiometry coefficients of reactant A in reactions (R 5-1) and (R 5-2) are ν_A and ν_B, respectively. In this study, the values of ν_A and ν_B are 1 and 2 (See reactions (R 4-1) and (R 4-7)). The above reaction can be rewritten as:

$$CO_2 + NH_3 \rightarrow products \qquad \text{(R 5-3)}$$

$$SO_2 + 2NH_3 \rightarrow products \quad \text{(R 5-4)}$$

Reaction (5-3) is the reaction between carbon dioxide and ammonia, which is pseudo-first-order reaction, and reaction (R 5-4) is the reaction between sulfur dioxide and ammonia, which is an instantaneous reaction.

5.2 Reaction Plane Model

The reaction between sulfur dioxide and ammonia is instantaneous reaction. Thus, the reaction occurs at a reaction plane[35].

When aqueous ammonia absorbs the sulfur dioxide, the following two-step reaction is taking place on the liquid side[41].

$$\mathrm{SO_2} + \mathrm{NH_3} + H_2O \rightleftharpoons NH_4^+ + HSO_3^- \quad \text{(R 5-5)}$$

$$HSO_3^- + \mathrm{NH_3} \rightleftarrows NH_4^+ + SO_3^{2-} \quad \text{(R 5-6)}$$

The values of equilibrium constants for reactions (R 5-5) and (R 5-6) are 3.1×10^7 and 1.1×10^2, respectively, at 25°C and infinite dilution[35]. Reaction (R 5-5) is considered as very fast, and reaction (R 5-6), which is a proton transfer reaction, is even much faster than reaction (R 5-5)[35]. Both reactions are thus considered as instantaneous reactions. Because both reactions (R 5-5) and (R 5-6) have very large equilibrium constants, the coexistence of the liquid-phase reactant $\mathrm{NH_3}$ with $\mathrm{SO_2}$ or the intermediate product HSO_3^- may be considered impossible.

$$K_1 = \frac{[NH_4^+][HSO_3^-]}{[\mathrm{SO_2}][\mathrm{NH_3}]} \quad \text{(5-1)}$$

$$K_2 = \frac{[NH_4^+][SO_3^{2-}]}{[HSO_3^-][\mathrm{NH_3}]} \quad \text{(5-2)}$$

Thus, the only species that can coexist with NH_3 are the final products of the reaction SO_3^{2-} and NH_4^+. However, in this two-step reaction, the ratio of equilibrium constant of the two reactions are:

$$\frac{K_1}{K_2} = \frac{[HSO_3^-]^2}{[\mathrm{SO_2}][SO_3^{2-}]} = 2.8 \times 10^5 \quad (5\text{-}3)$$

The ratio of equilibrium constant is the equilibrium constant for reaction:

$$SO_2 + SO_3^{2-} \rightleftharpoons 2HSO_3^- \quad (\mathrm{R}\ 5\text{-}7)$$

Thus coexisting of SO_2 and SO_3^{2-} can be considered as negligible because of a large equilibrium constant (5-3) and fast reaction of reactions (R 5-5) and (R 5-6). The species that could coexist with are the final products NH_4^+ and SO_3^{2-}. In this case, a three film theory is used to describe the mass transfer model; the two film theory is not suitable for this situation because there are two reactive regions in the liquid side film (one region for reaction with SO_2 and the other for reaction with CO_2).

Based on the case of sulfur dioxide and ammonia reaction, the diagram of concentration distribution of species in the liquid phase of simultaneous absorption of CO_2 and SO_2 in

NH3 is shown in Figure 5-1

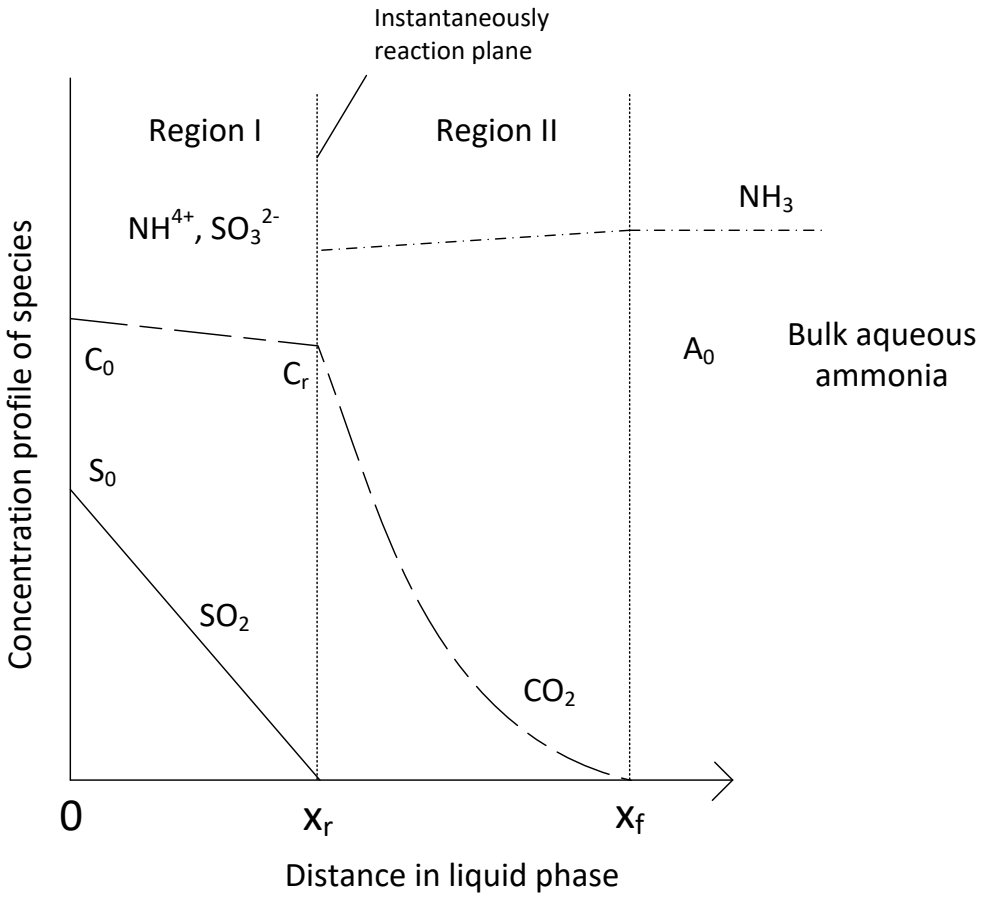

Figure 5-1Diagram of concentration distribution of species in liquid phase

In Figure 5-1, x_r is the distance from the interface to reaction plane. x_f is the thickness of the stagnate film, C_0 and S_0 are equilibrium concentrations of carbon dioxide and sulfur dioxide calculated by Henry's law at the interface. A_0 is the concentration of ammonia in the bulk liquid. C_r is the concentration of carbon dioxide in the reaction plane. Because of the absence of ammonia in the Region I, the reaction between carbon dioxide and ammonia in Region I will not take place. Thus, the carbon dioxide will only have diffusion in Region I, which can be described by Fick's first law:

$$N_{CO_2} = -D_{CO_2} \frac{dC_{CO_2}}{dx} \tag{5-4}$$

Where N_{CO_2} is molar mass flux of carbon dioxide

D_{CO_2} is the diffusion coefficient of carbon dioxide in aqueous ammonia, which can be calculated using (5-98) and (5-99)

C_{CO_2} is the concentration of carbon dioxide

x is the position, the dimension of which is length, x_r is the distance from interface to reaction plane. x_f is thickness of the stagnant film

In Region II, the ammonia is present. In that case, the reaction between ammonia and carbon dioxide will take place in Region II. Because of the absence of sulfur dioxide in Region II, there is no sulfur dioxide in Region II, the reaction between ammonia and sulfur dioxide will not happen in Region II. Since the sulfur dioxide diffuses only in Region I, the distance between the reaction plane and the interface is related to the equilibrium concentration of sulfur dioxide at the interface, which is related to the concentration of sulfur dioxide concentration in the gas phase. Thus, an increase in sulfur dioxide concentration in the bulk gas will increase the distance it takes to diffuse to the reaction plane. Besides, the reaction between sulfur dioxide and ammonia is rapid, and it can be assumed that there is no diffusion of ammonia ($\frac{dC_{NH_3}}{dx} = 0$) near the reaction plane ($x = {x_r}^+, {x_r}^-$).

The distance from the interface to the reaction plane has an effect on carbon dioxide absorption. Because of the distance from the interface to the reaction plane is changing with sulfur dioxide concentration in the bulk gas, the carbon dioxide concentration in reaction plane C_r is changing.

When the reaction between sulfur dioxide and the liquid-phase reactant ammonia is simultaneous, this reaction occurs at the reaction plane, where the concentrations of sulfur dioxide and ammonia are assumed zero. The mass flux of sulfur dioxide diffused to the reaction plane is twice that of the mass flux of ammonia (1 mole sulfur dioxide reacts with 2 mole ammonia according to reactions (R 5-5) and (R 5-6) .Thus, the relation of mass flux of sulfur dioxide and ammonia near the reaction plane is:

$$-v_B D_{SO_2}\left(\frac{dC_{SO_2}}{dx}\right) = D_{NH_3}\left(\frac{dC_{NH_3}}{dx}\right) \tag{5-5}$$

Carbon dioxide diffuses beyond the reaction plane and reacts with ammonia in the region between the reaction plane and the bulk aqueous ammonia.

The mass balance using film theory with chemical reaction and boundary conditions is described in the following

The mass balance of carbon dioxide over a thickness Δx of liquid phase, S of surface is:

$$N_{CO_2|x}S - N_{CO_2|x+\Delta x}S - k_{CO_2}C_{CO_2}C_{NH_3}S\Delta x = 0 \tag{5-6}$$

$$\frac{dN_{CO_2}}{dz} + k_{CO_2}C_{CO_2}C_{NH_3} = 0 \tag{5-7}$$

$$N_{CO_2} = -D_{\mathrm{CO_2}}\frac{dC_{CO_2}}{dx} \tag{5-8}$$

Combining the last two equations gives:

$$D_{\mathrm{CO_2}}\frac{d^2C_{CO_2}}{dx^2} = k_{CO_2}C_{CO_2}C_{NH_3} \tag{5-9}$$

The mass balance for sulfur dioxide and ammonia can be derived similarly and gives:

$$D_{SO_2}\frac{d^2C_{SO_2}}{dx^2} = k_{SO_2}C_{SO_2}C_{NH_3} \tag{5-10}$$

$$D_{NH_3}\frac{d^2C_{NH_3}}{dx^2} = k_{CO_2}C_{CO_2}C_{NH_3} + 2k_{SO_2}C_{SO_2}C_{NH_3} \tag{5-11}$$

Where the reaction constant k_{CO_2} can be calculated by equation (4-52)

The derivation for the enhancement factor of carbon dioxide absorbed by ammonia is based on the work of Hikita[39], as shown in Appendix B.

However, the derivation in the derivation in Hikita's article cannot be approached by the derivation shown in Appendix B- Analytical solution of mass transfer of CO_2 in ammonia. The reason is the different assumption with linearized concentration profile of carbon dioxide in region $x_r < x < x_f$. The article derived the following equation by assuming linearized concentration profile of carbon dioxide in region$x_r < x < x_f$:

$$\mathrm{A} = \left(\frac{dA}{dx}\right)_{x=x_r}(x - x_r) + A_r = (A_r - A_i)\frac{x}{x_r} + A_i \tag{5-12}$$

This indicated that the equation is only true when x=x_r so that this equation can't be used to solve other equations with x≠x_r. In that case, the analytical solution is difficult for this complicated reaction situation. Thus, equations (5-9) to (5-11) have to be solved numerically, as shown in section 5.3.

5.3 Numerical Calculation

The equations describing diffusion and reaction between the interface at x=0 and the film boundary condition at $x = x_f$ were discussed above from equations (5-4) to (5-8). The diffusion with chemical reaction of carbon dioxide and sulfur dioxide in aqueous ammonia are shown in equations (5-9) and (5-10)

The boundary conditions are shown in equations (5-13) to (5-15):

x=0 $$C_{CO_2}=C_0,\ C_{SO_2}=S_0 \tag{5-13}$$

x=x_r $$C_{CO_2}=C_r,\ C_{SO_2}=0,\ C_{NH_3}=0,\ -2D_{\mathrm{CO_2}}\left(\frac{dC_{SO_2}}{dx}\right)=D_{CO_2}\left(\frac{dC_{NH_3}}{dx}\right) \tag{5-14}$$

x=x_f $$\frac{dC_{CO_2}}{dx}=0,\ C_{CO_2}=0,\ C_{SO_2}=0,\ C_{NH_3}=A_0 \tag{5-15}$$

Because the reaction between sulfur dioxide and ammonia is instantaneous, so the reaction constant $k_{SO_2}$is considered infinite.

Dimensionless forms were used to simplify the numerical solution:

Both sides of equation (5-12) were divided by $D_{CO_2}C_0A_0\left(\frac{1}{x_f}\right)^2$ which leads to:

$$\frac{d^2\frac{C_{CO_2}}{C_0}}{d\left(\frac{x}{x_f}\right)^2}=\frac{A_0k_{CO_2}{x_f}^2}{\mathrm{D}_{CO_2}}\frac{C_{CO_2}}{C_0}\frac{C_{NH_3}}{A_0} \tag{5-16}$$

Define the following dimensionless parameters:

$$c=\frac{C_{CO_2}}{C_0},\ a=\frac{C_{NH_3}}{A_0},\ \xi=\frac{x}{x_f},\ Ha^2=\frac{k_{CO_2}A_0{x_f}^2}{\mathrm{D}_{CO_2}} \tag{5-17}$$

This yields the following dimensionless equation:

$$\frac{d^2c}{d\xi^2}=Ha^2c\mathrm{a} \tag{5-18}$$

The dimensionless parameter Ha in equation (5-18) is called the Hatta number:

$$Ha=x_f\sqrt{\frac{k_{CO_2}A_0}{\mathrm{D}_{CO_2}}} \tag{5-19}$$

Recall equation:

$$k_L = \frac{D_L}{\delta_L} \tag{5-20}$$

The thickness of the liquid film δ_L is equal to x_f, which was discussed in section 5.2, and the diffusion coefficient D_L is the diffusion coefficient of carbon dioxide in aqueous ammonia D_{CO_2} , which is related to the overall mass transfer coefficient through equation 5-23.:

$$k_L = \frac{\mathrm{D}_{CO_2}}{x_f} \tag{5-21}$$

Substitute equation (5-21) to eliminate x_f in equation (5-19):

$$Ha = \frac{\sqrt{k_{CO_2}\mathrm{D}_{CO_2}A_0}}{k_L} \tag{5-22}$$

In Chapter 4 the reaction between carbon dioxide and ammonia is considered as pseudo-first-order reaction with respect to carbon dioxide for the determination of the enhancement factor from experimental data, and where the concentration of ammonia is assumed unchanged. Then, Equation (5-10) becomes:

$$\mathrm{D}_{CO_2-NH_3}\frac{d^2C_{CO_2}}{dx^2} = k_{CO_2}C_{CO_2} \tag{5-23}$$

The Hatta number of this pseudo-first-order reaction can be derived by a similar process from equation (5-16) to (5-22) and gives:

$$\frac{d^2c}{d\xi^2} = Ha^2c \tag{5-24}$$

$$Ha = \frac{\sqrt{k_{CO_2} \mathrm{D}_{CO_2}}}{k_L} \tag{5-25}$$

The general solution of equation (5-24) is:

$$c = C_1 \cosh Ha\xi + C_2 \sinh Ha\xi \tag{5-26}$$

Apply the boundary condition c=1, $\xi = 0$ shown in (5-44) :

$$1 = C_1 \cosh Ha * 0 + C_2 \sinh Ha * 0 \tag{5-27}$$

$$1 = C_1 \tag{5-28}$$

Take derivation on both sides of equation (5-26) and apply the other boundary condition $\frac{dc}{d\xi} = 0, \xi = 1$ in (5-44):

$$\frac{dc}{d\xi} = HaC_1 \sinh Ha\xi + HaC_2 \cosh Ha\xi \tag{5-29}$$

$$0 = C_1 \sinh Ha + C_2 \cosh Ha \tag{5-30}$$

$$0 = \sinh Ha + C_2 \cosh Ha \tag{5-31}$$

$$C_2 = -\frac{\sinh Ha}{\cosh Ha} \tag{5-32}$$

Apply (5-28) and (5-32) to equation(5-26) to have:

$$c = \frac{\cosh Ha \cosh Ha\xi - \sinh Ha \sinh Ha\xi}{\cosh Ha} = \frac{\cosh[Ha(1-\xi)]}{\cosh Ha} \tag{5-33}$$

Reverting to the original notation for c:

$$\frac{C_{CO_2}}{C_0} = \frac{\cosh[Ha(1-\xi)]}{\cosh Ha} \tag{5-34}$$

The concentration profile can thus be obtained by equation (5-34). The molar flux N_{CO_2} can be found by applying equation (5-47) to (5-4):

$$N_{CO_2} = -\mathrm{D}_{CO_2}\frac{dC_{CO_2}}{dx} = \frac{d\frac{C_0\cosh[Ha(1-\xi)]}{\cosh Ha}}{dx} \tag{5-35}$$

$$N_{CO_2} = C_0\frac{D_{CO_2}}{x_f}Ha\tanh Ha \tag{5-36}$$

The equation (5-36) will not be used in numerical calculation in this work but shows the derivative process of equation (3-19) used in section 3.4.Thus the flux calculated here is at x=x_f. Applying equation (5-21) to (5-36) and obtains the expression of the mass flux of carbon dioxide as a function of the Hatta number:

$$N_{CO_2} = C_0 k_L Ha\tanh Ha \tag{5-37}$$

Similarly, Equation (5-10) was converted to a dimensionless form by dividing by $\mathrm{D}_{SO_2-NH_3}S_0A_0(\frac{1}{x_f})^2$:

$$\frac{d^2\frac{C_{SO_2}}{S_0}}{d(\frac{x}{x_f})^2} = \frac{A_0k_{SO_2}{x_f}^2}{D_{SO_2}}\frac{C_{SO_2}}{S_0}\frac{C_{NH_3}}{A_0} \tag{5-38}$$

Multiplying both sides by $\frac{D_{SO_2}}{D_{CO_2}}$ and multiplying the right side by $\frac{k_{CO_2}}{k_{CO_2}}$ yields:

$$\frac{D_{SO_2}}{D_{CO_2}}\frac{d^2\frac{C_{SO_2}}{S_0}}{d(\frac{x}{x_f})^2} = \frac{k_{SO_2}}{k_{CO_2}}\frac{A_0k_{CO_2}{x_f}^2}{D_{CO_2}}\frac{C_{SO_2}}{S_0}\frac{C_{NH_3}}{A_0} \tag{5-39}$$

Given the dimensionless parameters:

$$r_{SO_2} = \frac{\mathrm{D}_{SO_2}}{\mathrm{D}_{CO_2}}, p = \frac{k_{SO_2}}{k_{CO_2}}, s = \frac{C_{SO_2}}{S_0} \tag{5-40}$$

The equation converted to the following dimensionless form:

$$r_{SO_2}\left(\frac{d^2s}{d\xi^2}\right) = pHa^2sa \tag{5-41}$$

Equation (5-11) was converted to a dimensionless form in a similar way to obtain:

$$r_{NH_3}\left(\frac{d^2a}{d\xi^2}\right) = Ha^2(m_C ca + pm_S sa) \tag{5-42}$$

Where:

$$r_{NH_3} = \frac{D_{NH_3}}{D_{CO_2}} \tag{5-43}$$

With dimensionless boundary conditions

$$c(0) = 1 \qquad c(1) = 0 \qquad \frac{dc}{d(1)} = 0 \tag{5-44}$$

$$s(0) = 1 \qquad s(1) = 0 \tag{5-45}$$

$$\frac{da}{d\xi}(0) = 0 \qquad a(1) = 1 \tag{5-46}$$

Where:

$$c = \frac{C_{CO_2}}{C_0}, s = \frac{C_{SO_2}}{S_0}, a = \frac{C_{NH_3}}{A_0}\, p = \frac{k_{SO_2}}{k_{CO_2}} \tag{5-47}$$

$$m_c = \frac{v_C C_0}{A_0},\ m_s = \frac{v_S S_0}{A_0}, \xi = \frac{x}{x_L}, Ha^2 = \frac{k_C A_0 {x_L}^2}{D_{CO_2}} = \frac{k_C A_0 D_{CO_2}}{k_L^2} \tag{5-48}$$

$$r_s = \frac{D_{SO_2}}{D_{CO_2}}, r_A = \frac{D_{NH_3}}{D_{CO_2}} \tag{5-49}$$

As discussed in section 5.2 there is a reaction plane in this model because of the infinitely fast reaction between sulfur dioxide and ammonia. Thus, p is infinite. Rearranging equation (5-41) :

$$\lim_{p\to\infty} sa = \lim_{p\to\infty} \left(\frac{r_S}{Ha^2 p}\right)\left(\frac{d^2 s}{d\xi^2}\right) = 0 \tag{5-50}$$

Which suggests the existence of a reaction plane at $\xi = \xi^*$ so that:

$$\text{A=0 at } 0 \leq \xi \leq \xi^* \tag{5-51}$$

$$\text{S=0 at } \xi^* \leq \xi \leq 1 \tag{5-52}$$

In Region I there is no reaction of carbon dioxide, According to Fick's law(5-4) the concentration profiles are linear so that the reaction factor for carbon dioxide, E_C, can be calculated by equations (B-9) to (B-12) in Appendix B with dimensionless forms as follows:

$$E_C = \frac{dc}{d\xi} \tag{5-53}$$

$$E_C = \frac{(1 - c^*)}{\xi^*} \tag{5-54}$$

The reaction factor for sulfur dioxide E_S is:

$$E_S = \frac{1}{\xi^*} \tag{5-55}$$

Where:

$$c^* = c(\xi^*) \tag{5-56}$$

There is no reaction between sulfur dioxide and ammonia in the region $\xi^* \leq \xi \leq 1$ so equation (5-42) becomes:

$$r_A\left(\frac{d^2a}{d\xi^2}\right) = Ha^2 m_C ca \tag{5-57}$$

Subject equation (5-18) to the above equation with boundary conditions:

$$c(\xi^*) = c^*, c(1) = 0 \tag{5-58}$$

$$a(\xi^*) = 0, a(1) = 1 \tag{5-59}$$

We have:

$$\frac{r_A}{m_C}\left(\frac{d^2a}{d\xi^2}\right) = \frac{d^2c}{d\xi^2} \tag{5-60}$$

$$\frac{r_A}{m_C}\left(\frac{d^2a}{d\xi^2}\right) - \frac{d^2c}{d\xi^2} = 0 \tag{5-61}$$

$$\int\left[\frac{r_A}{m_C}\left(\frac{d^2a}{d\xi^2}\right) - \frac{d^2c}{d\xi^2}\right] = 0 \tag{5-62}$$

$$\frac{r_A}{m_C}\left(\frac{da}{d\xi}\right) - \frac{dc}{d\xi} = C_1 \tag{5-63}$$

$$\int\left[\frac{r_A}{m_C}\left(\frac{da}{d\xi}\right) - \frac{dc}{d\xi}\right] = \int C_1 \tag{5-64}$$

$$\frac{r_A}{m_C}a - c = C_1\xi + C_2 \tag{5-65}$$

Apply the boundary condition (5-58) and (5-59) to equation (5-65):

$$-c^* = c_1\xi^* + c_2 \tag{5-66}$$

$$\frac{r_A}{m_C} = c_1 + c_2 \tag{5-67}$$

(5-66) - (5-67):

$$-c^* - \frac{r_A}{m_C} = c_1(\xi^* - 1) \tag{5-68}$$

$$c_1 = -\frac{c^* + \frac{r_A}{m_C}}{\xi^* - 1} \tag{5-69}$$

Multiply both sides of equation (5-67) with ξ^*:

$$\frac{r_A}{m_C}\xi^* = c_1\xi^* + c_2\xi^* \tag{5-70}$$

(5-70)-(5-67):

$$\frac{r_A}{m_C}\xi^* + c^* = c_2\xi^* - c_2 = c_2(\xi^* - 1) \tag{5-71}$$

$$c_2 = \frac{\frac{r_A}{m_C}\xi^* + c^*}{\xi^* - 1} \tag{5-72}$$

Replace the c_1, c_2 in equation (5-65) with their expression in equations (5-69) and (5-69):

$$\frac{r_A}{m_C}a - c = -\frac{c^* + \frac{r_A}{m_C}}{\xi^* - 1}\xi + \frac{\frac{r_A}{m_C}\xi^* + c^*}{\xi^* - 1} \tag{5-73}$$

Multiply by m_C:

$$r_A a - m_C c = -\frac{m_C c^* + r_A}{\xi^* - 1}\xi + \frac{r_A \xi^* + m_C c^*}{\xi^* - 1} \tag{5-74}$$

$$r_A a - m_C c = \frac{r_A \xi^* + m_C c^* - (m_C c^* + r_A)\xi}{\xi^* - 1} \tag{5-75}$$

Because of no reaction between carbon dioxide and ammonia in the Region I (Figure 5-1), the distribution of concentration of carbon dioxide is linear respect to the dimension of , thus:

$$\frac{dc}{d\xi} = \frac{dc}{d\xi(0)} = -\frac{1 - c^*}{\xi^*} \tag{5-76}$$

Moreover, $\frac{dc}{d\xi}$ is continuous across the reaction plane.

Because of the reaction between ammonia and sulfur dioxide is complete, the molar flux of sulfur dioxide diffused to reaction plane: $N_S = D_{SO_2}\frac{dC_{SO_2}}{dx(x_r{}^-)}$ is equal to the negative molar flux of ammonia diffused to the reaction plane: $N_A = D_{NH_3}\frac{dA}{dx(x_r{}^+)}$ The mass balance at the reaction plane can be written as:

$$-N_S{}^{x_r{}^-} = N_A{}^{x_r{}^+} \tag{5-77}$$

$$-D_{SO_2} S_0 \frac{d\frac{C_{SO_2}}{S_0}}{dx(x_r{}^-)} = D_{NH_3} A_0 \frac{d\frac{C_{NH_3}}{A_0}}{dx(x_r{}^+)} \tag{5-78}$$

$$-\frac{D_{SO_2}}{D_{CO_2}} S_0 \frac{d\frac{C_{SO_2}}{S_0}}{dx(x_r{}^-)} = \frac{D_{NH_3}}{D_{CO_2}} A_0 \frac{d\frac{C_{NH_3}}{A_0}}{dx(x_r{}^+)} \tag{5-79}$$

$$\frac{D_{SO_2}}{D_{CO_2}}\frac{S_0}{A_0}\frac{d\frac{C_{SO_2}}{S_0}}{d\frac{x}{x_L},(x_r{}^-)}=\frac{D_{NH_3}}{D_{CO_2}}\frac{d\frac{C_{NH_3}}{A_0}}{d\frac{x}{x_L},(x_r{}^+)} \tag{5-80}$$

Apply equations (5-47) to (5-49) to convert the above equation (5-80) to dimensionless form:

$$r_A\frac{dA}{d\xi(\xi^{*+})}=-r_s m_s\frac{ds}{d\xi(\xi^{*-})} \tag{5-81}$$

The concentration of sulfur dioxide distribution in Region I is linear so the derivative of sulfur dioxide concentration is the slope of the concentration:

$$r_A\frac{dA}{d\xi(\xi^{*+})}=-r_s m_s\frac{ds}{d\xi(\xi^{*-})}=\frac{r_s m_s}{\xi^*} \tag{5-82}$$

Differentiating equation (5-75):

$$m_C\frac{dc}{d\xi}-r_A\frac{da}{d\xi}=\frac{-(m_C c^*+r_A)}{1-\xi^*} \tag{5-83}$$

Apply equation (5-76) and (5-81) to eliminate the differentiation equation (5-83):

$$m_C\frac{c^*-1}{\xi^*}-\frac{r_S m_S}{\xi^*}=-\frac{m_C c^*+r_A}{1-\xi^*} \tag{5-84}$$

$$m_C(c^*-1)(1-\xi^*)-r_S m_S(1-\xi^*)=-m_C c^*-r_A \tag{5-85}$$

$$\begin{aligned} m_C(c^*-c^*\xi^*-1+\xi^*)-r_S m_S(1-\xi^*) \\ =-m_C c^*-r_A \end{aligned} \tag{5-86}$$

$$m_C c^* = m_C + r_S m_S - (m_C + r_S m_S + r_A)\xi^* \quad (5\text{-}87)$$

Equation (5-87) shows the relation between $c^*$and ξ^*. The numerical solution can be obtained by giving input value of continuous value to m_C in equations (5-18) and enhancement factor E_C in (5-53) and check if the solution is satisfying the boundary conditions (5-58) and (5-59). The value of enhancement factor without chemical reaction E_C is compared with the value of enhancement factor with chemical reaction, E, calculated with Matlab. Because of the consistent concentration distribution of carbon dioxide near the reaction plane, the value of enhancement factor without chemical reaction E_C and the value of enhancement factor with chemical reaction E is equal. The value of Ha is calculated by solving the boundary value problem with the input value of $\xi^*$from 0 to 1. Thus, the relation between Ha and ξ^* can be found. Further, with experimental data, the value of Ha could be determined thus, the ξ^*can be calculated. Once $\xi^*$is known, the concentration profile in Region 2, as well as the flux of CO_2 can be calculated, which in turn can be used to predict the experimental data.

The boundary value problem was solved numerically with Matlab. The process of solving the boundary value problem is shown in Figure 5-2:

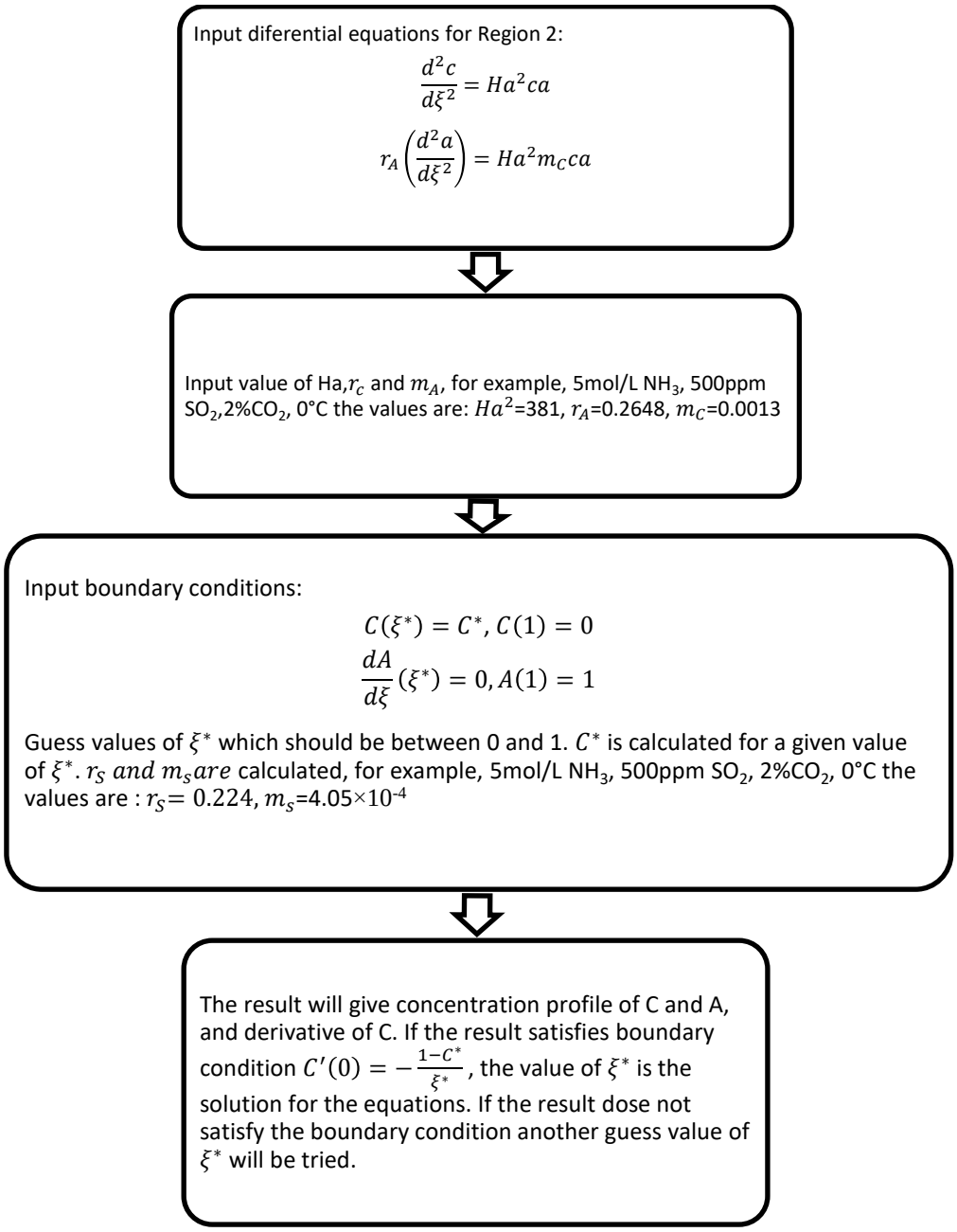

Figure 5-2 Numerical calculation process

The enhancement factor E calculated by the numerical method will be used to calculate the mass flux of the carbon dioxide absorbed by ammonia.

The mass flux of carbon dioxide absorbed into liquid phase can be calculated by:

$$N_{CO_2} = -D_{CO_2} \frac{dC_{CO_2}}{dx} \tag{5-88}$$

The thickness x_f of film can be found by definition:

$$k_L = \frac{D_{CO_2-NH_3}}{x_f} \tag{5-89}$$

Dimensionless concentration of carbon dioxide:

$$C = \frac{C_{CO_2}}{C_0} \tag{5-90}$$

The derivative of dimensionless concentration of carbon dioxide is as follows:

$$\frac{dC}{d\xi} = \frac{d\frac{C_{CO_2}}{C_{CO_2-interface}}}{d\frac{x}{x_f}} = \frac{dC_{CO_2}}{dx}\frac{x_f}{C_{CO_2-interface}} \tag{5-91}$$

$$\frac{dC_{CO_2}}{dx} = \frac{dC}{d\xi}\frac{C_{CO_2-interface}}{x_f} = \frac{dC}{d\xi}\frac{C_{CO_2-interface}}{\frac{D_{CO_2-NH_3}}{k_L}} \tag{5-92}$$

Substitute equation (5-92) into equation (5-88) to eliminate $\frac{dC_{CO_2}}{dx}$:

$$N_{CO_2} = -D_{CO_2-NH_3}\frac{dC}{d\xi}\frac{C_{CO_2-interface}}{\frac{D_{CO_2-NH_3}}{k_L}} \tag{5-93}$$

The calculation of the diffusion coefficient and other physicochemical properties has been discussed in section 5.4. Thus, the numerically calculated molar flux of carbon

dioxide absorbed by ammonia N_{CO_2} can be calculated. The Matlab code can be found in Appendix A- Matlab code for Various Calculations.

The mass flux of carbon dioxide absorbed by ammonia in the presence of sulfur dioxide N_{CO_2} calculated in this section will be used to compare with the mass flux from Appendix C- Experimental data. The results are presented in Figure 6-1 in section 6.1.

To predict the mass transfer with sulfur dioxide presenting in carbon dioxide absorption in experimental data, a simplified calculation of the mass flux of carbon dioxide absorbed by ammonia in Region II in Figure 5-1, carbon dioxide concentration in $x = x_r$ with assumption that the carbon dioxide concentration in bulk ammonia is 0 can be used. Because the carbon dioxide have chemical reaction with ammonia only in Region II in Figure 5-1 the mass flux can be calculated by equation (4-8). The ratio of mass flux determined by experiment without sulfur dioxide N_{CO_2} and with sulfur dioxide N_{CO_2,SO_2} is as follows:

$$\frac{N_{CO_2,SO_2}}{N_{CO_2}} = \frac{Ek_L(C_{lb} - C_r)}{Ek_L(C_{lb} - C_0)} \tag{5-94}$$

The concentration of carbon dioxide in bulk liquid can be considered as 0 since all carbon dioxide will reacts with ammonia. The equation (5-94) becomes:

$$\frac{N_{CO_2,SO_2}}{N_{CO_2}} = \frac{C_r}{C_0} \tag{5-95}$$

$$N_{CO_2,SO_2} = \frac{C_r N_{CO_2}}{C_0} \tag{5-96}$$

Thus, to predict the experimental determined mass flux of carbon dioxide absorbed into aqueous ammonia with sulfur dioxide presenting, the equation (5-96) can be used. The ratio of carbon dioxide concentration in different condition $\frac{C_r}{C_0}$ can be calculated with a simplified model (6-6) which will be discussed in section 6.2. The value of mass flux

determined by experiment without sulfur dioxide N_{CO_2} can be determined experimentally. The overall mass transfer coefficient can be determined similarly:

$$\frac{K_{G-CO_2,SO_2}}{K_G} = \frac{N_{CO_2,SO_2}(P^*_{gb} - P_{gb})}{N_{CO_2}(P^*_{gb} - P_{gb})} = \frac{N_{CO_2,SO_2}}{N_{CO_2}} = \frac{C_r}{C_0} \tag{5-97}$$

The equation (5-97) will be used to compare the numerical model in this work with other's results, which will be shown in section 6.2.

5.4 Physicochemical Properties

The diffusivities of CO_2 and SO_2 in aqueous ammonia solutions is correlated with its viscosity by the modified Stokes-Einstein equation as follows[31]:

$$D_{CO_2} = D_{CO_2-H_2O}\left(\frac{\mu_{H_2O}}{\mu NH_3}\right)^{0.8} \tag{5-98}$$

$$D_{SO_2} = D_{SO_2-H_2O}\left(\frac{\mu_{H_2O}}{\mu NH_3}\right)^{0.8} \tag{5-99}$$

The diffusivity of NH_3 in water can be well predicted by the Wilke-Chang equation[42]

$$D_{NH_3} = 7.4 \times 10^{-8}(\gamma M_{H_2O})^{0.5}\frac{T}{\mu_{H_2O}V_b^{0.6}} \tag{5-100}$$

Where

$D_{CO_2-H_2O}$ is liquid-phase diffusivity of dissolved carbon dioxide in water, $m^2\ s^{-1}$

$D_{SO_2-H_2O}$ is liquid-phase diffusivity of dissolved sulfur dioxide in water, $m^2\ s^{-1}$

M: molecular weight of solvent.

γ: association parameter

μ_{H_2O}: Viscosity of water, Pa s

μ_{NH_3}: viscosity of ammonia, Pa s

V_b: molar volume of solute at its normal boiling temperature, $cm^3\ mol^{-1}$

T: temperature, K.

The viscosity of an aqueous ammonia solution depends on the concentration of NH_3 and temperature, and can be estimated by the following correlation[43]:

$$\mu_{NH_3} = (0.67 + 0.78x_{NH_3}) \times 10^{-6} e^{\frac{17900}{RT}} \quad (5\text{-}101)$$

The mole fraction of NH_3 in water x_{NH_3} can be calculated by the relationship between molar concentration and mole fraction of ammonia as proposed by Jennings[44].

$$C_{NH_3} = -30.36x_{NH_3}^2 + 72.3x_{NH_3} - 0.806 \quad (5\text{-}102)$$

The diffusivity of CO_2 in water is studied by Geert[45]. The value of diffusivity of CO_2 in water $D_{CO_2-H_2O}$ is corrected to $1.6\times10^{-9}\ m^2\ s^{-1}$ and SO_2 in water $D_{SO_2-H_2O}$ is $2.3\times10^{-9}\ m^2\ s^{-1}$ under temperature 280K. Because the experiment is done with temperature around 273K, the above values of diffusivity are reasonable to be used.[42]

As the dimensions of the reactor in this study were almost the same as those in Sada's works[46, 47] and stirring speeds for both phases were close to theirs, their empirical correlations for gas-liquid mass transfer coefficients were employed. Firstly, the liquid-

phase mass transfer coefficient of carbon dioxide and the gas-phase mass transfer coefficient are correlated with corresponding stirring speed as:

$$k_{L,CO_2-H_2O} = 9.41 \times 10^{-7} n_L^{0.65} \quad (5\text{-}103)$$

Where

k_{L,CO_2-H_2O} is liquid-phase mass transfer coefficient of carbon dioxide in water m s^{-1}

n_L is liquid-phase stirring speed n_L, rpm

The temperature dependence of Henry's constant can be calculated by:

$$H_c = H_c^{\ominus} \times \exp\left(\frac{\Delta_{solv}H}{R}\left(\frac{1}{T} - \frac{1}{T^{\ominus}}\right)\right) \quad (5\text{-}104)$$

Where $\Delta_{solv}H$ is enthalpy of solution,

$H_c^{\ominus}$ is Henry's law constant of carbon dioxide refer to standard conditions (T=298.15K)

$T^{\ominus}$ =298.15K

The values of enthalpy of solution can be found in Sander's study[48].

By applying the physicochemical properties to the equations in section 5.3, the results of the numerical model can be found. The results of numerical model and the comparison between the experimental data and numerical model will be discussed in Chapter 6.

Chapter 6 Results and Discussion

6.1 Effects of SO_2 Concentration on CO_2 Mass Transfer

Figure 6-1 shows the result of the experiment of the SO_2 effect on CO_2 absorption with aqueous ammonia. The result shows the negative effect of sulfur dioxide on CO_2 absorption by aqueous ammonia. The mass flux of CO_2 absorbed by ammonia is decreasing with increasing the concentration of sulfur dioxide in the gas phase with ammonia concentration from 1mol/L to 6 mol/L. The mass flux of CO_2 absorbed by 1mol/L ammonia solution dropped from 1.21×10^{-10} mol cm^{-2} s^{-1} to 0.66×10^{-10} mol cm^{-2} s^{-1}. The figure shows that when the concentration of ammonia is 6 mol/l the decreasing of mass flux of CO_2 is slightly slower (mass flux dropped from 2.59×10^{-10} mol cm^{-2} s^{-1} to 2.07×10^{-10} mol cm^{-2} s^{-1}) than that it is absorbed by $1\ mol \cdot L^{-1}$ ammonia. The decreasing in mass flux of CO_2 caused by the presence of SO_2 is not affected much by the concentration of ammonia. The experimentally determined mass transfer coefficients shown in Appendix C- Experimental data are in same order of magnitude as those in Qin et al. work[25]. However, the temperature range in the experiments of Qi's work was 20 to 80 °C, which is higher for chilled ammonia process (0-20°C). Thus, one needs to be aware of the temperature differences when comparing the mass transfer coefficients obtained from Qi's work and those obtained in the present work. In Qi's work, the relation between the effects of sulfur dioxide on carbon dioxide mass transfer and the temperature is not stated. In this work, the effects of sulfur dioxide on mass transfer of carbon dioxide not depend much on temperature (at least in temperature range 0-80 °C). The dash lines in Figure 6-1 are results performed by the numerical model. The numerical model fits well with the experimental data. The numerical model represents well the decreasing in the mass flux of carbon dioxide absorbed by ammonia when the sulfur dioxide concentration in the gas stream is increased. The numerical model can be used to estimate the effects of sulfur dioxide on carbon dioxide.

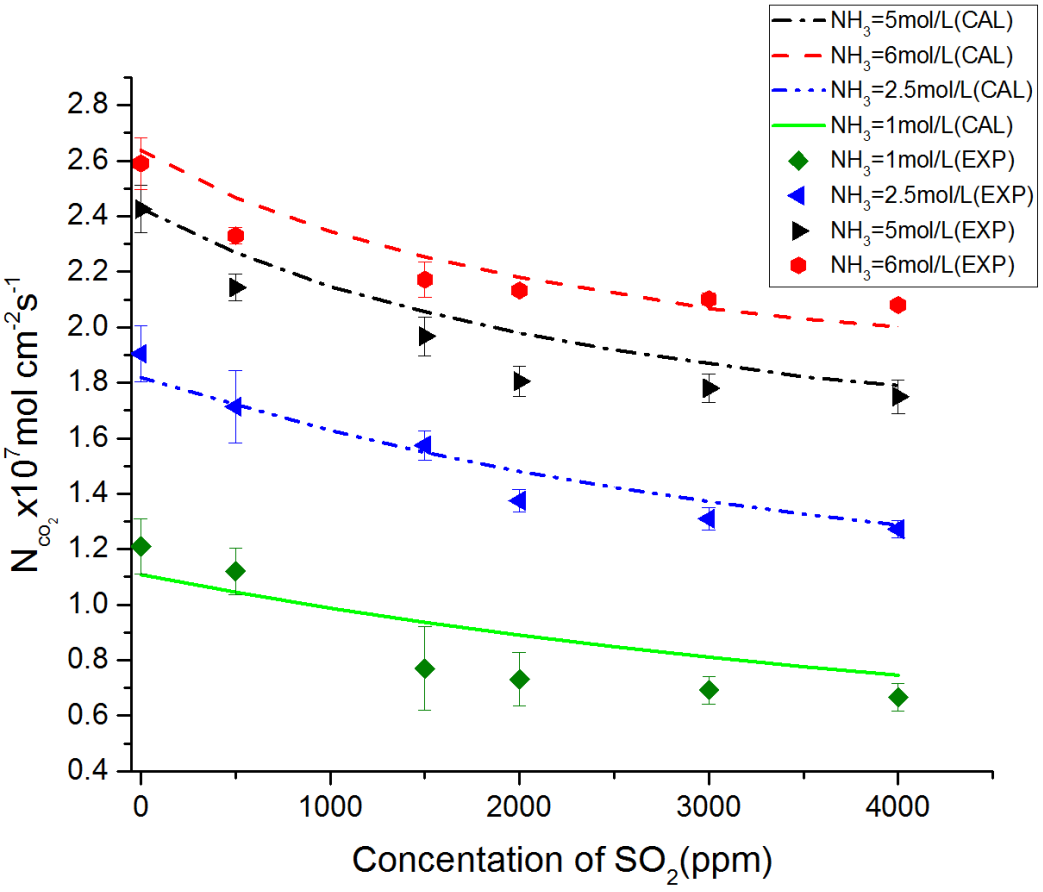

Figure 6-1 Experimental data and numerical calculation results of sulfur dioxide effect on carbon dioxide mass flux

6.2 General Equation by Fitting the Numerical Solution

In the absence of SO_2, only Region II would exist. Region I is due to the presence of SO_2 where SO_2 reacts instantaneously with NH_3, thus forming a gradient of concentration in a region where water is presenting but not NH_3 (See Figure 5-1). As mentioned previously, the main effect of SO_2 is thus to affect the thickness of Region II, which in turn affects the concentration of CO_2 at the reaction interface. Indeed, the carbon dioxide concentration at the reaction interface will decrease as the thickness of Region I increasing. Because of the complexity of calculation of the concentration profiles of SO_2

and CO_2, e.g. if one want to perform a process simulation of the entire system, this section attempts to derive a simpler, but accurate relationship for estimating the carbon dioxide mass flux in the presence sulfur dioxide. The fitting of the numerical model was created by polynomial fitting using Origin, as shown in Figure 6-2. Polynomial fitting of sulfur dioxide concentration and concentration of carbon dioxide in reaction plane can be used to estimate the mass flux of carbon dioxide absorbed by ammonia when the ammonia concentrations are 1, 2.5, 5, 6 $mol \cdot L^{-1}$. The equation and R^2 values are shown in Table 6-1. The R^2 values are between 0.986 and 0.998.

However, the estimation of carbon dioxide flux with theffects of sulfur dioxide for various ammonia concentrations (1, 2.5, 5, and 6 $mol \cdot L^{-1}$) is limited. A more general equation is required. Thus, effect of ammonia concentration on carbon dioxide concentration at the reaction plane $C_r was$ plotted, as shown in Figure 6-3. The ammonia concentration does not seem to have much effect on the way CO_2 decreases when increasing SO_2 concentrations. Except for the lowest NH_3 concentration, the profile of CO_2 dimensionless concentration at the reaction plane is weakly affected by NH_3 concentration. The carbon dioxide concentration in the reaction plane was calculated using the numerical program shown in Appendix A- Matlab code for Various Calculations.

The concentration of carbon dioxide in the reaction plane C_r shown in Figure 5-1 can be predicted byfunction $f(S_0)$as the ratio of C_r and C_0:

$$C_r = f(S_0)C_0 \tag{6-1}$$

The function of S_0, $f(S_0)$is given by polynomial regressionby each line shown in Figure 6-3 which were calculated by equation (6-1). The values of R^2 for these four different ammonia concentrations are ranging from 0.990 to 0.999. A summary of

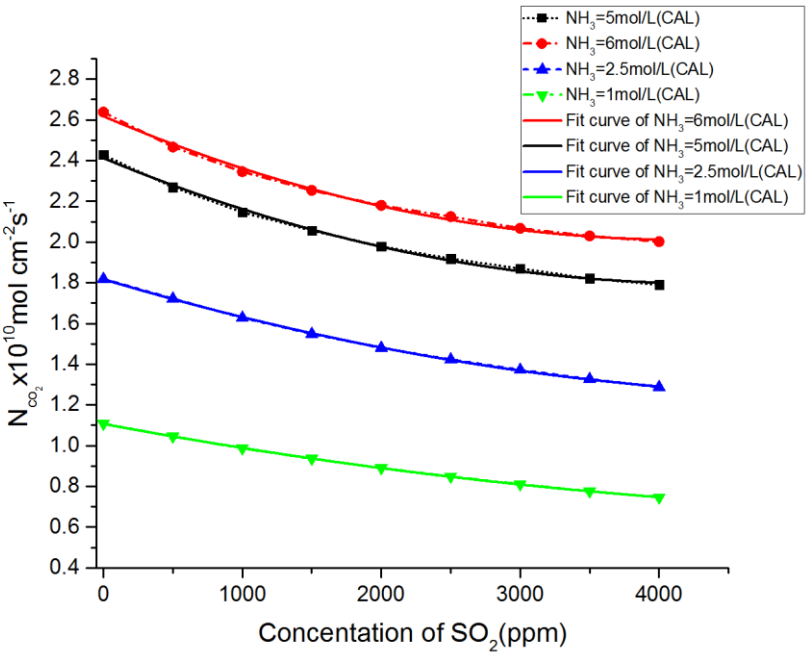

Figure 6-2 Polynomial fitting of numerical calculation results

parameters of optimal fitting are shown in Table 6-2. To calculate the mass flux of carbon dioxide with equation (3-19), C_r will be used instead of C_0 in equation (6-1)as

Table 6-1 Summary of optimal fitting parameters for numerical results of mass flux of CO_2 absorbed into ammonia

Equation	N_{CO_2}= Intercept + $B_1 S_0$ + $B_2 x {S_0}^2$ (6-2)			
Plot	1 $mol \cdot L^{-1}$	2.5 $mol \cdot L^{-1}$	5 $mol \cdot L^{-1}$	6 $mol \cdot L^{-1}$
Intercept	1.106563	1.87769	2.41198	2.61756

B_1	-1.27E-04× 10^{-4}	-2.03× 10^{-4}	-2.82× 10^{-4}	-2.90× 10^{-4}
B_2	1.61× 10^{-8}	1.894× 10^{-8}-	3.239× 10^{-8}	3.470× 10^{-8}
Adj.R-Square	0.98604	0.99892	0.99619	0.995

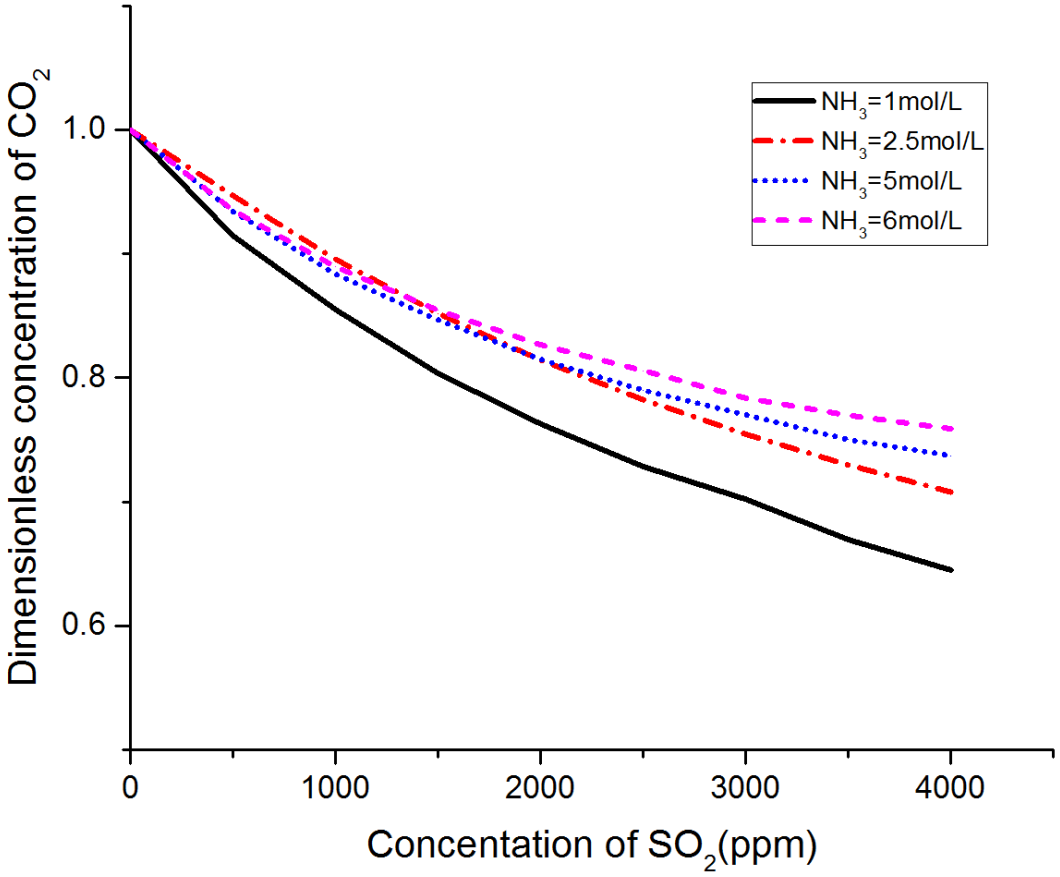

Figure 6-3 Dimensionless concentration of CO_2 in reaction plane

carbon dioxide concentration that will react with ammonia. Figure 6-3 shows a negative effect of ammonia concentration on sulfur dioxide effect on mass transfer of carbon dioxide absorbed by ammonia.

Table 6-2 The Summary of optimal fitting parameters for numerical results of dimensionless concentration of CO_2 in reaction plane

Equation	$f(S_0)$ = Intercept + $B_1 S_0$ + $B_2 {S_0}^2$ (6-3)			
plot	1 $mol \cdot L^{-1}$	2.5 $mol \cdot L^{-1}$	5 $mol \cdot L^{-1}$	6 $mol \cdot L^{-1}$
Intercept	1	1	1	1
B_1	-1.52× 10^{-4}	-1.221 × 10^{-4}	-1.20110^{-4}	-1.17× 10^{-4}
B_2	1.45× 10^{-8}	1.46× 10^{-8}	1.00× 10^{-8}	1.64× 10^{-8}
Adj.R-Square	0.99542	0.99971	0.9962	0.995

The parameter B_1 in Table 6-2 is decreasing when increasing the ammonia solution concentration. The difference of calculated values of dimensionless carbon dioxide in Figure 6-3 mainly depend on the values of B_1 because the absolute values of $B_1 S_0$ are larger than $B_2 {S_0}^2$. Others parameters like B_2 and intercepts in Table 6-2 are not found to change significantly with ammonia concentration. Thus, the parameter B_1 can be described by a function of concentration of ammonia solution. A nonlinear curve fit was performed by using Origin, and the B_1 as function of ammonia concentration is shown in Figure 6-4:

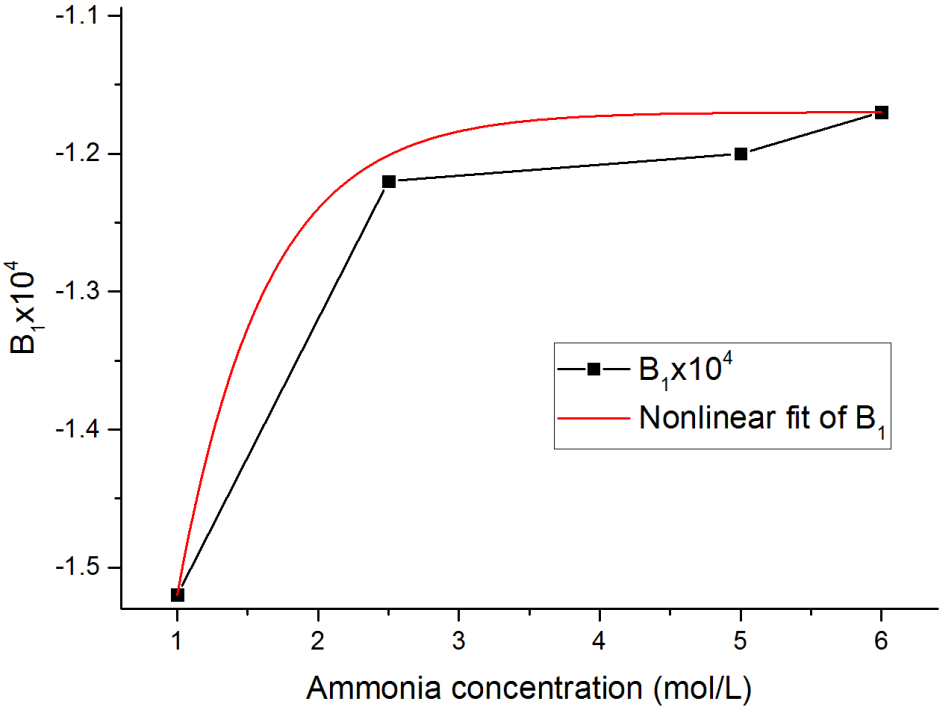

Figure 6-4 B_1 value as function of ammonia concentration

The equation of the fitting of ammonia concentration and B_1 in Figure 6-4 is shown in equation (6-4). The R-square for this fitting is 0.94057.

$$B_1 = \left(-2.92744 + 1.75 * \left(1 - \exp\left(-\frac{C_{NH_3}}{0.6213}\right)\right)\right) \times 10^4 \tag{6-4}$$

Substitute $f(C_{SO_2}^{gb})$ in equation (6-1) with equation (6-3) to have:

$$C_r = (1 + B_1 S_0 + B_2 {S_0}^2) C_0 \tag{6-5}$$

Substitute B_1 in equation (6-5) with equation (6-4) and average value of intercept and B_2 in Table 6-2 to have the general expression of effect of sulfur dioxide on carbon dioxide concentration in reaction plane, which described in section 5.2:

$$C_r = \left(1 + \left(-2.92744 + 1.75 * \left(1 - \exp\left(-\frac{C_{NH_3}}{0.6213}\right)\right)\right) S_0 \times 10^{-4} + 1.2525 \times 10^{-8} {S_0}^2\right) C_0 \quad (6\text{-}6)$$

The model was used to compare the results using the "general" equation with Qi's work, using equation (5-97). The results are shown in Figure 6-5. The model fits the result of Qi's work well except at high SO_2 concentrations and higher temperatures. The experimental conditions in Qi's work were different from those in this work (most notably the temperature).

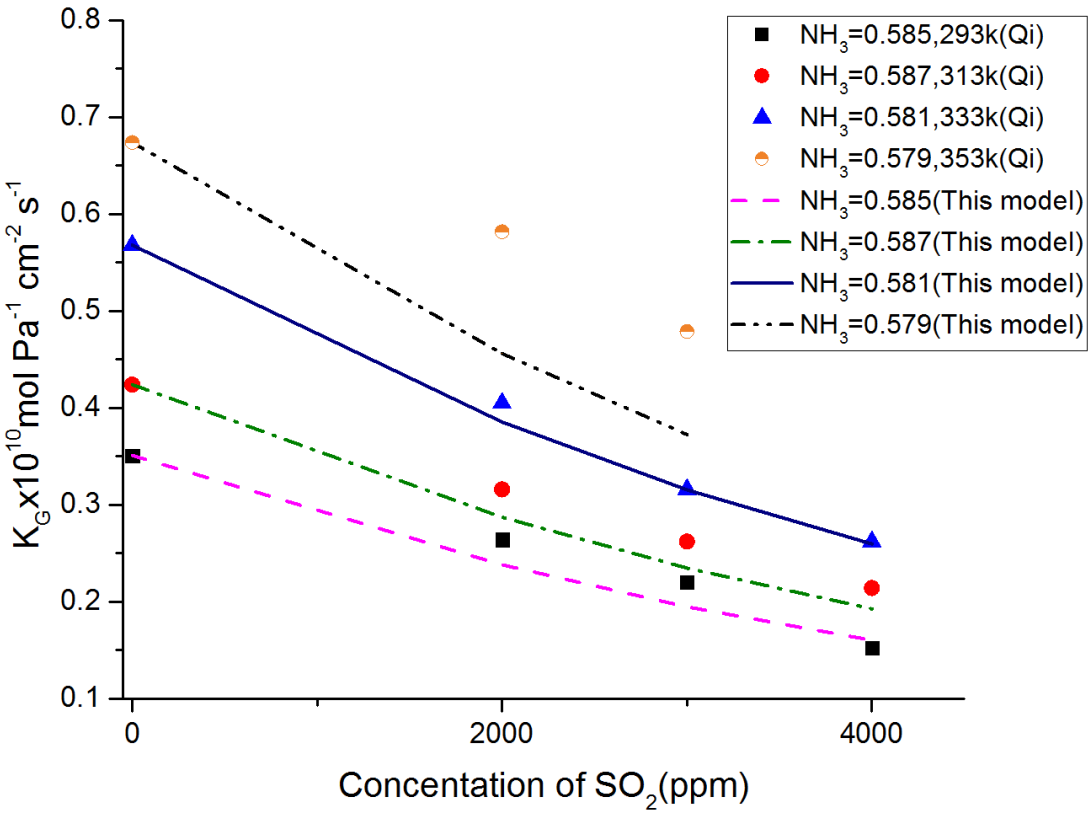

Figure 6-5 Comparison of mass transfer coefficients to the work of Qi.

Nonetheless, it is remarkable to see that the correlation in this work, which was developed at a temperature of 0°C, represents well experimental data generated by

another group and for temperatures up to 60°C and for SO_2 concentrations up to 4000ppm (at 60°C, the fit is good up to SO_2 concentration of 2000 ppm). Thus, with equation (6-6), the molar mass flux of carbon dioxide absorbed by aqueous ammonia with sulfur dioxide presenting can be calculated by using the concentration of carbon dioxide in reaction plane (C_r) instead of concentration in the interface (C_0) in equation (3-19). All the results from the experiment and modeling give a conclusion in general that the sulfur dioxide have negative effects on carbon dioxide mass transfer into aqueous ammonia and the effects of sulfur dioxide can be quantified with the model presented in this work.

Chapter 7 Conclusions and Recommendations

From an industrial implication point of view, the closer the value of C_0 to C_r the higher the flux of carbon dioxide will be captured by aqueous ammonia. Thus, the sulfur dioxide needs to be removed before the carbon dioxide capture process when using aqueous ammonia as absorbent. However, there are still residues sulfur dioxide after FGD process to proceed to carbon dioxide capture; the flue gas will proceed to desulfurize before the carbon dioxide capture. The higher concentration of aqueous ammonia used to capture carbon dioxide the less the sulfur dioxide negative effects on carbon dioxide mass transfer which can be seen from the equation (6-6) either. The increasing of concentration of aqueous ammonia (C_{NH_3}) will lead to the increasing of the coefficient of C_0 to C_r. While the increasing concentration of aqueous ammonia may also increase the volatilization, which may cause increasing of FGD equipment cost[49] either. The equation (6-6) can be used to quantify the change of carbon flux absorbed into aqueous ammonia caused by sulfur dioxide concentration and ammonia concentration change. Thus, the overall benefit of larger carbon dioxide capture flux by increasing ammonia concentration and FGD equipment can be estimated. The optimized carbon dioxide capture operation condition can be predicted, and the balance point of the energy and material cost between the larger carbon capture capacity and larger cost to maintain high concentration ammonia absorbent and high-efficiency FGD equipment can be found. There are also some limits to this model. The temperature of the experiment in this work is around 0°C.

Because the model is fitted to experimental data, the mass flux measured under the certain temperature will limit the use of the model from other temperature that the model will have more when predicting the problem with temperature much different from 0°C,even Henry's constant can be corrected by equation (5-104). Although there are

much kinetic and mass transfer research on carbon dioxide capture with aqueous ammonia[2, 25, 30, 31], they were performed without the sulfur dioxide existing. The effects of sulfur dioxide on carbon dioxide capture by aqueous ammonia is novel research area, there are not much available studies to compare with. This work not only filled up the blank of quantity study of sulfur dioxide effects on carbon dioxide capture using chilled ammonia process but also introduced a model to the study of sulfur dioxide effects on carbon dioxide capture with aqueous ammonia. The model can be used in the similar study that related with flue gases effect on carbon dioxide capture either, like the effect of sulfur dioxide and nitric oxide. While the research on temperature effect is relatively important in future work. Because of volatilization of ammonia varies with temperature[50], a system study of both temperature and sulfur dioxide effect will bring this model closer to real-word problems. This model can be optimized in future study to predict not only sulfur dioxide and ammonia concentration but also nitric oxide, temperature and even the volatilization of aqueous ammonia effects.

Bibliography

1 EuropeanCom- mission, 'Emission Database for Global Atmospheric Research(Edgar) ⟨http://edgar.jrc.ec.europa.eu/overview.php?v⟩ '.

2 Zhongchao Tan, *Air Pollution and Greenhouse Gases: From Basic Concepts to Engineering Applications for Air Emission Control* (Springer, 2014).

3 Nicola Marsh, B. Belaissaoui, D. Willson, and E. Favre, 'Euromembrane Conference 2012 Post–combustion Carbon Dioxide Capture using Membrane Processes: A Sensitivity Analysis', *Procedia Engineering*, 44 (2012), 1191-95.

4 Shan Zhou, Shujuan Wang, and Changhe Chen, 'Thermal Degradation of Monoethanolamine in CO_2 Capture with Acidic Impurities in Flue Gas', *Industrial & Engineering Chemistry Research*, 51 (2012), 2539-47.

5 A Dehghani, and H Bridjanian, 'Flue gas desulfurization methods to conserve the environment', *Petroleum & Coal*, 52 (2010), 220-26.

6 Margaret R Taylor, Edward S Rubin, and David A Hounshell, 'Control of SO_2 Emissions from Power Plants: A Case of Induced Technological Innovation in The US', *Technological Forecasting and Social Change*, 72 (2005), 697-718.

7 Victor Darde, Kaj Thomsen, Willy J. M. van Well, and Erling H. Stenby, 'Chilled ammonia process for CO_2 capture', *International Journal of Greenhouse Gas Control*, 4 (2010), 131-36.

8 Eliane Blomen, Chris Hendriks, and Filip Neele, 'Capture Technologies: Improvements and Promising Developments', *Energy Procedia*, 1 (2009), 1505-12.

9 Robert M Davidson, *Post-combustion Carbon Capture From Coal Fired Plants: Solvent Scrubbing* (IEA Clean Coal Centre London, 2007).

10 BJP Buhre, LK Elliott, CD Sheng, RP Gupta, and TF Wall, 'Oxy-fuel Combustion Technology for Coal-Fired Power Generation', *Progress in energy and combustion science*, 31 (2005), 283-307.

11 Imo Pfaff, and Alfons Kather, 'Comparative Thermodynamic Analysis and Integration Issues of CCS Steam Power Plants Based on Oxy-Combustion with Cryogenic or Membrane Based Air Separation', *Energy Procedia*, 1 (2009), 495-502.

12 Deanna M D'Alessandro, Berend Smit, and Jeffrey R Long, 'Carbon Dioxide Capture: Prospects for New Materials', *Angewandte Chemie International Edition*, 49 (2010), 6058-82.

13 Abass A. Olajire, 'CO_2 Capture and Separation Technologies for End-of-Pipe Applications – A Review', *Energy*, 35 (2010), 2610-28.

14 Dumitru Cebrucean, Viorica Cebrucean, and Ioana Ionel, 'CO_2 Capture and Storage from Fossil Fuel Power Plants', *Energy Procedia*, 63 (2014), 18-26.

15 Burcu E Gurkan, Juan C de la Fuente, Elaine M Mindrup, Lindsay E Ficke, Brett F Goodrich, Erica A Price, William F Schneider, and Joan F Brennecke, 'Equimolar CO_2 Absorption by Anion-Functionalized Ionic Liquids', *Journal of the American Chemical Society*, 132 (2010), 2116-17.

16 Yukihiro Takamura, Junya Aoki, Shigeo Uchida, and Saburou Narita, 'Application of High-Pressure Swing Adsorption Process for Improvement of CO_2 Recovery System From Flue Gas', *The Canadian Journal of Chemical Engineering*, 79 (2001), 812-16.

17 Ambarish R. Kulkarni, and David S. Sholl, 'Analysis of Equilibrium-Based TSA Processes for Direct Capture of CO_2 from Air', *Industrial & Engineering Chemistry Research,* 51 (2012), 8631-45.
18 J. Adánez, L. F. de Diego, F. García-Labiano, P. Gayán, A. Abad, and J. M. Palacios, 'Selection of Oxygen Carriers for Chemical-Looping Combustion', *Energy & Fuels,* 18 (2004), 371-77.
19 Qamar Zafar, Tobias Mattisson, and Börje Gevert, 'Integrated Hydrogen and Power Production with CO_2 Capture Using Chemical-Looping Reformingredox Reactivity of Particles of CuO, Mn_2O_3, NiO, and Fe_2O_3 Using SiO_2 as A Support', *Industrial & Engineering Chemistry Research,* 44 (2005), 3485-96.
20 Prakash D Vaidya, and Eugeny Y Kenig, 'CO_2 - Alkanolamine Reaction Kinetics: A Review of Recent Studies', *Chemical Engineering & Technology,* 30 (2007), 1467-74.
21 Praveen Linga, Rajnish Kumar, and Peter Englezos, 'The Clathrate Hydrate Process for Post and Pre-Combustion Capture of Carbon Dioxide', *Journal of Hazardous Materials,* 149 (2007), 625-29.
22 P. Englezos, Ripmeester, J. A., Kumar, R., & Linga, P., 'Hydrate Processes for CO_2 Capture and Scale Up Using A New Apparatus', (2008, July 31).
23 L. C. Elwell, and W. S. Grant, 'Technology Options for Capturing CO_2', *Power,* 150 (2006), 60-65.
24 Dennis Y. C. Leung, Giorgio Caramanna, and M. Mercedes Maroto-Valer, 'An Overview of Current Status of Carbon Dioxide Capture and Storage Technologies', *Renewable and Sustainable Energy Reviews,* 39 (2014), 426-43.
25 Guojie Qi, Shujuan Wang, Zhicheng Xu, Bo Zhao, and Changhe Chen, 'Mass Transfer and Kinetics Study on Combined CO_2 And SO_2 Absorption Using Aqueous Ammonia', *International Journal of Greenhouse Gas Control,* 41 (2015), 60-67.
26 Feng Qin, Shujuan Wang, Ardi Hartono, Hallvard F Svendsen, and Changhe Chen, 'Kinetics of CO_2 Absorption in Aqueous Ammonia Solution', *International Journal of Greenhouse Gas Control,* 4 (2010), 729-38.
27 W. P. M. van Swaaij, and G. F. Versteeg, 'Mass Transfer Accompanied with Complex Reversible Chemical Reactions in Gas—Liquid Systems: An Overview', *Chemical Engineering Science,* 47 (1992), 3181-95.
28 Theodore L Bergman, Frank P Incropera, and Adrienne S Lavine, *Fundamentals of Heat and Mass Transfer* (John Wiley & Sons, 2011).
29 S Hatta, 'On the Absorption Velocity of Gases by Liquids', *Tech. Repts. Tohoku Imp. Univ,* 10 (1932), 119-28.
30 Michael Caplow, 'Kinetics of Carbamate Formation and Breakdown', *Journal of the American Chemical Society,* 90 (1968), 6795-803.
31 P. W. J. Derks, and G. F. Versteeg, 'Kinetics of Absorption of Carbon Dioxide in Aqueous Ammonia Solutions', *Energy Procedia,* 1 (2009), 1139-46.
32 Haruo Hikita, Satoru Asai, and Tadashi Tsuji, 'Absorption of Sulfur Dioxide into Aqueous Sodium Hydroxide and Sodium Sulfite Solutions ', *AIChE Journal,* 23 (1977), 538-44.
33 W. G. Whitman, 'Preliminary experimental confirmation of the two-film theory of gas absorption', *Chem. Metall. Eng.,* 29 (1923), 146-8.

34 Victor Darde, Willy JM Van Well, Philip L Fosboel, Erling H Stenby, and Kaj Thomsen, 'Experimental Measurement and Modeling of The Rate of Absorption of Carbon Dioxide by Aqueous Ammonia', *International Journal of Greenhouse Gas Control*, 5 (2011), 1149-62.
35 H. Hikita, S. Asai, and T. Tsuji, 'Absorption of Sulfur-Dioxide into Aqueous Ammonia and Ammonium Sulfite Solutions', *Journal Of Chemical Engineering Of Japan*, 11 (1978), 236-38.
36 BRW Pinsent, L Pearson, and FJW Roughton, 'The Kinetics of Combination of Carbon Dioxide with Ammonia', *Transactions of the Faraday Society*, 52 (1956), 1594-98.
37 Hesheng Yu, Zhongchao Tan, Xianshe Feng, Eric Croiset, Jesse Thé, and William A Anderson, 'Kinetics of The Absorption of Carbon Dioxide into Aqueous Ammonia Solutions', *AIChE Journal* (2016).
38 P. A. Ramachandran, 'Simultaneous Absorption of Two Gases Accompanied by Reversible Instantaneous Chemical Reactions', *Chemical Engineering Science*, 26 (1971), 349-55.
39 H. Hikita, S. Asai, and H. Ishikawa, 'Simultaneous Absorption of 2 Gases in A Reactive Liquid, One Gas Reacting Instantaneously', *Chemical Engineering Journal And the Biochemical Engineering Journal*, 18 (1979), 169-72.
40 Lloyd A. Goettler, and Robert L. Pigford, 'Computational Studies of The Simultaneous Chemical Absorption of Two Gases', *AIChE Journal*, 17 (1971), 793-800.
41 Haruo Hikita, Satoru Asai, and Tadashi Tsuji, 'Absorption of Sulfur Dioxide into Aqueous Sodium Hydroxide and Sodium Sulfite Solutions', *AIChE Journal*, 23 (1977), 538-44.
42 CR Wilke, and Pin Chang, 'Correlation of Diffusion Coefficients in Dilute Solutions', *AIChE Journal*, 1 (1955), 264-70.
43 Marco J. W. Frank, Johannes A. M. Kuipers, and Wim P. M. van Swaaij, 'Diffusion Coefficients and Viscosities of $CO_2 + H_2O$, $CO_2 + CH_3OH$, $NH_3 + H_2O$, and $NH_3 + CH_3OH$ Liquid Mixtures', *Journal of Chemical & Engineering Data*, 41 (1996), 297-302.
44 Burgess H Jennings, and Francis Patrick Shannon, *Tables of The Properties of Aqua-ammonia Solutions: Part 1 of The Thermodynamics of Absorption Refrigeration* (Lehigh University, 1938).
45 Geert F. Versteeg, and Wlm Van Swaalj, 'Solubility and Diffusivity of Acid Gases (Carbon Dioxide, Nitrous Oxide) in Aqueous Alkanolamine Solutions', *Journal of Chemical & Engineering Data*, 33 (1988), 29-34.
46 Eizo Sada, Hidehiro Kumazawa, Ichibeiv Kudo, and Takashi Kondo, 'Individual and Simultaneous Absorption of Dilute NO and SO_2 in Aqueous Slurries of $MgSO_3$ with FeII-EDTA', *Industrial & Engineering Chemistry Process Design and Development*, 19 (1980), 377-82.
47 Eizo Sada, Hidehiro Kumazawa, Norio Tsubol, Ichibei Kudo, and Takashi Kondo, 'Absorption of Nitric Oxide in Aqueous Ferrous Sulfate Solutions', *Industrial & Engineering Chemistry Process Design and Development*, 17 (1978), 321-24.
48 Rolf Sander, 'Compilation of Henry's Law Constants for Inorganic and Organic Species of Potential Importance in Environmental Chemistry', (Max-Planck Institute of Chemistry, Air Chemistry Department Mainz, Germany, 1999).
49 Patricia Córdoba, 'Status of Flue Gas Desulphurisation (FGD) Systems from Coal-Fired Power Plants: Overview of The Physic-Chemical Control Processes of Wet Limestone FGDS', *Fuel*, 144 (2015), 274-86.
50 A. A. Shaikh, and A. Varma, 'Gas Absorption with Chemical Reaction: The Case Involving A Volatile Liquid Reactant', *Chemical Engineering Science*, 39 (1984), 1639-41.

A. Appendix A- Matlab code for Various Calculations

A. Viscosity of water

```
function viscosity_H2O

vW_0=1.18*10.^-6*exp(16400/(8.314*273))

vW_10=1.18*10.^-6*exp(16400/(8.314*283))

vW_20=1.18*10.^-6*exp(16400/(8.314*293))

vW_0=vpa(vW_0,10)

vW_10=vpa(vW_10,10)

vW_20=vpa(vW_20,10)
```

B. Diffusion coefficient of carbon dioxide in ammonia solution calculation:

```
function diffuCN

global M x y x1 x2 x5 x6 DCN

x=[0:0.0001:0.2]

y=-29.208*x.^2+72.392*x-0.8041

M=1

tmp = abs(y-M)

[idx idx]= min(tmp)

closest=y(idx)

Frac1= find(y==closest)

x1=x(Frac1)
```

```
M=2.5

tmp = abs(y-M)

[idx idx]= min(tmp)

closest=y(idx)

Frac1= find(y==closest)

x2=x(Frac1)

M=5

tmp = abs(y-M)

[idx idx]= min(tmp)

closest=y(idx)

Frac1= find(y==closest)

x5=x(Frac1)

M=6

tmp = abs(y-M)

[idx idx]= min(tmp)

closest=y(idx)

Frac1= find(y==closest)

x6=x(Frac1)

global v_1_0 v_2_0 v_5_0 v_6_0 v_1_10 v_2_10 v_5_10 v_6_10 v_1_20 v_2_20
v_5_20 v_6_20

v_1_0=(0.67+0.78*x1)*10.^-6*exp(17900/8.314/273)

v_2_0=(0.67+0.78*x2)*10.^-6*exp(17900/8.314/273)

v_5_0=(0.67+0.78*x5)*10.^-6*exp(17900/8.314/273)

v_6_0=(0.67+0.78*x6)*10.^-6*exp(17900/8.314/273)

v_1_10=(0.67+0.78*x1)*10.^-6*exp(17900/8.314/283)

v_2_10=(0.67+0.78*x2)*10.^-6*exp(17900/8.314/283)
```

```
v_5_10=(0.67+0.78*x5)*10.^-6*exp(17900/8.314/283)

v_6_10=(0.67+0.78*x6)*10.^-6*exp(17900/8.314/283)

v_1_20=(0.67+0.78*x1)*10.^-6*exp(17900/8.314/293)

v_2_20=(0.67+0.78*x2)*10.^-6*exp(17900/8.314/293)

v_5_20=(0.67+0.78*x5)*10.^-6*exp(17900/8.314/293)

v_6_20=(0.67+0.78*x6)*10.^-6*exp(17900/8.314/293)

v_1_0=vpa(v_1_0,10)

v_2_0=vpa(v_2_0,10)

v_5_0=vpa(v_5_0,10)

v_6_0=vpa(v_6_0,10)

v_1_10=vpa(v_1_10,10)

v_2_10=vpa(v_2_10,10)

v_5_10=vpa(v_5_10,10)

v_6_10=vpa(v_6_10,10)

v_1_20=vpa(v_1_20,10)

v_2_20=vpa(v_2_20,10)

v_5_20=vpa(v_5_20,10)

v_6_20=vpa(v_6_20,10)

global vW_0 vW_10 vW_20

vW_0=1.18*10.^-6*exp(16400/(8.314*273))

vW_10=1.18*10.^-6*exp(16400/(8.314*283))

vW_20=1.18*10.^-6*exp(16400/(8.314*293))

vW_0=vpa(vW_0,10)

vW_10=vpa(vW_10,10)

vW_20=vpa(vW_20,10)
```

```
diffCN_1_0=1.6*10.^-9*(vW_0/v_1_0).^0.8;
diffCN_2_0=1.6*10.^-9*(vW_0/v_2_0).^0.8;
diffCN_5_0=1.6*10.^-9*(vW_0/v_5_0).^0.8;
diffCN_6_0=1.6*10.^-9*(vW_0/v_6_0).^0.8;
diffCN_1_10=1.6*10.^-9*(vW_10/v_1_10).^0.8;
diffCN_2_10=1.6*10.^-9*(vW_10/v_2_10).^0.8;
diffCN_5_10=1.6*10.^-9*(vW_10/v_5_10).^0.8;
diffCN_6_10=1.6*10.^-9*(vW_10/v_6_10).^0.8;
diffCN_1_20=1.6*10.^-9*(vW_20/v_1_20).^0.8;
diffCN_2_20=1.6*10.^-9*(vW_20/v_2_20).^0.8;
diffCN_5_20=1.6*10.^-9*(vW_20/v_5_20).^0.8;
diffCN_6_20=1.6*10.^-9*(vW_20/v_6_20).^0.8;
DCN=[
diffCN_1_0
diffCN_2_0
diffCN_5_0
diffCN_6_0
diffCN_1_10
diffCN_2_10
diffCN_5_10
diffCN_6_10
diffCN_1_20
diffCN_2_20
diffCN_5_20
diffCN_6_20]
```

```
DCN
```

C. Diffusion coefficient of sulfur dioxide in ammonia solution calculation:

```
function DiffuSN
global M x y x1 x2 x5 x6 DSN
x=[0:0.0001:0.2]
y=-29.208*x.^2+72.392*x-0.8041
M=1
tmp = abs(y-M)
[idx idx]= min(tmp)
closest=y(idx)
Frac1= find(y==closest)
x1=x(Frac1)
M=2.5
tmp = abs(y-M)
[idx idx]= min(tmp)
closest=y(idx)
Frac1= find(y==closest)
x2=x(Frac1)
M=5
tmp = abs(y-M)
[idx idx]= min(tmp)
closest=y(idx)
Frac1= find(y==closest)
x5=x(Frac1)
```

```
M=6

tmp = abs(y-M)

[idx idx]= min(tmp)

closest=y(idx)

Frac1= find(y==closest)

x6=x(Frac1)

global v_1_0 v_2_0 v_5_0 v_6_0 v_1_10 v_2_10 v_5_10 v_6_10 v_1_20 v_2_20
v_5_20 v_6_20

v_1_0=(0.67+0.78*x1)*10.^-6*exp(17900/8.314/273)

v_2_0=(0.67+0.78*x2)*10.^-6*exp(17900/8.314/273)

v_5_0=(0.67+0.78*x5)*10.^-6*exp(17900/8.314/273)

v_6_0=(0.67+0.78*x6)*10.^-6*exp(17900/8.314/273)

v_1_10=(0.67+0.78*x1)*10.^-6*exp(17900/8.314/283)

v_2_10=(0.67+0.78*x2)*10.^-6*exp(17900/8.314/283)

v_5_10=(0.67+0.78*x5)*10.^-6*exp(17900/8.314/283)

v_6_10=(0.67+0.78*x6)*10.^-6*exp(17900/8.314/283)

v_1_20=(0.67+0.78*x1)*10.^-6*exp(17900/8.314/293)

v_2_20=(0.67+0.78*x2)*10.^-6*exp(17900/8.314/293)

v_5_20=(0.67+0.78*x5)*10.^-6*exp(17900/8.314/293)

v_6_20=(0.67+0.78*x6)*10.^-6*exp(17900/8.314/293)

v_1_0=vpa(v_1_0,10)

v_2_0=vpa(v_2_0,10)

v_5_0=vpa(v_5_0,10)

v_6_0=vpa(v_6_0,10)

v_1_10=vpa(v_1_10,10)

v_2_10=vpa(v_2_10,10)
```

```
v_5_10=vpa(v_5_10,10)

v_6_10=vpa(v_6_10,10)

v_1_20=vpa(v_1_20,10)

v_2_20=vpa(v_2_20,10)

v_5_20=vpa(v_5_20,10)

v_6_20=vpa(v_6_20,10)

global vW_0 vW_10 vW_20

vW_0=1.18*10.^-6*exp(16400/(8.314*273))

vW_10=1.18*10.^-6*exp(16400/(8.314*283))

vW_20=1.18*10.^-6*exp(16400/(8.314*293))

vW_0=vpa(vW_0,10)

vW_10=vpa(vW_10,10)

vW_20=vpa(vW_20,10)

diffSN_1_0=2.32*10.^-9*(vW_0/v_1_0).^0.8;

diffSN_2_0=2.32*10.^-9*(vW_0/v_2_0).^0.8;

diffSN_5_0=2.32*10.^-9*(vW_0/v_5_0).^0.8;

diffSN_6_0=2.32*10.^-9*(vW_0/v_6_0).^0.8;

diffSN_1_10=2.32*10.^-9*(vW_10/v_1_10).^0.8;

diffSN_2_10=2.32*10.^-9*(vW_10/v_2_10).^0.8;

diffSN_5_10=2.32*10.^-9*(vW_10/v_5_10).^0.8;

diffSN_6_10=2.32*10.^-9*(vW_10/v_6_10).^0.8;

diffSN_1_20=2.32*10.^-9*(vW_20/v_1_20).^0.8;

diffSN_2_20=2.32*10.^-9*(vW_20/v_2_20).^0.8;

diffSN_5_20=2.32*10.^-9*(vW_20/v_5_20).^0.8;

diffSN_6_20=2.32*10.^-9*(vW_20/v_6_20).^0.8;
```

```
DSN=[

diffSN_1_0

diffSN_2_0

diffSN_5_0

diffSN_6_0

diffSN_1_10

diffSN_2_10

diffSN_5_10

diffSN_6_10

diffSN_1_20

diffSN_2_20

diffSN_5_20

diffSN_6_20]

DSN
```

Fraction .

D. Viscosity of ammonia water

```
function viscosity_NH

syms M x y x1 x2 x5 x6

x=[0:0.0001:0.2]

y=-29.208*x.^2+72.392*x-0.8041

M=1

tmp = abs(y-M)

[idx idx]= min(tmp)

closest=y(idx)

Frac1= find(y==closest)
```

```
x1=x(Frac1)

M=2.5

tmp = abs(y-M)

[idx idx]= min(tmp)

closest=y(idx)

Frac1= find(y==closest)

x2=x(Frac1)

M=5

tmp = abs(y-M)

[idx idx]= min(tmp)

closest=y(idx)

Frac1= find(y==closest)

x5=x(Frac1)

M=6

tmp = abs(y-M)

[idx idx]= min(tmp)

closest=y(idx)

Frac1= find(y==closest)

x6=x(Frac1)


v_1_0=(0.67+0.78*x1)*10.^-6*exp(17900/8.314/273)

v_2_0=(0.67+0.78*x2)*10.^-6*exp(17900/8.314/273)

v_5_0=(0.67+0.78*x5)*10.^-6*exp(17900/8.314/273)

v_6_0=(0.67+0.78*x6)*10.^-6*exp(17900/8.314/273)

v_1_10=(0.67+0.78*x1)*10.^-6*exp(17900/8.314/283)
```

```
v_2_10=(0.67+0.78*x2)*10.^-6*exp(17900/8.314/283)

v_5_10=(0.67+0.78*x5)*10.^-6*exp(17900/8.314/283)

v_6_10=(0.67+0.78*x6)*10.^-6*exp(17900/8.314/283)

v_1_20=(0.67+0.78*x1)*10.^-6*exp(17900/8.314/293)

v_2_20=(0.67+0.78*x2)*10.^-6*exp(17900/8.314/293)

v_5_20=(0.67+0.78*x5)*10.^-6*exp(17900/8.314/293)

v_6_20=(0.67+0.78*x6)*10.^-6*exp(17900/8.314/293)

v_1_0=vpa(v_1_0,10)

v_2_0=vpa(v_2_0,10)

v_5_0=vpa(v_5_0,10)

v_6_0=vpa(v_6_0,10)

v_1_10=vpa(v_1_10,10)

v_2_10=vpa(v_2_10,10)

v_5_10=vpa(v_5_10,10)

v_6_10=vpa(v_6_10,10)

v_1_20=vpa(v_1_20,10)

v_2_20=vpa(v_2_20,10)

v_5_20=vpa(v_5_20,10)

v_6_20=vpa(v_6_20,10)
```

E. Diffusion coefficient of ammonia in water:

```
function diffunw

global M x y x1 x2 x5 x6 DNW
```

```
x=[0:0.0001:0.2]
y=-29.208*x.^2+72.392*x-0.8041
M=1
tmp = abs(y-M)
[idx idx]= min(tmp)
closest=y(idx)
Frac1= find(y==closest)
x1=x(Frac1)
M=2.5
tmp = abs(y-M)
[idx idx]= min(tmp)
closest=y(idx)
Frac1= find(y==closest)
x2=x(Frac1)
M=5
tmp = abs(y-M)
[idx idx]= min(tmp)
closest=y(idx)
Frac1= find(y==closest)
x5=x(Frac1)
M=6
tmp = abs(y-M)
[idx idx]= min(tmp)
closest=y(idx)
Frac1= find(y==closest)
```

```
x6=x(Frac1)


diffNW_1_0=(1.65+2.74*x1)*10.^-6*exp(-16600/8.314/273)
diffNW_1_10=(1.65+2.74*x1)*10.^-6*exp(-16600/8.314/283)
diffNW_1_20=(1.65+2.74*x1)*10.^-6*exp(-16600/8.314/293)
diffNW_2_0=(1.65+2.74*x2)*10.^-6*exp(-16600/8.314/273)
diffNW_2_10=(1.65+2.74*x2)*10.^-6*exp(-16600/8.314/283)
diffNW_2_20=(1.65+2.74*x2)*10.^-6*exp(-16600/8.314/293)
diffNW_5_0=(1.65+2.74*x5)*10.^-6*exp(-16600/8.314/273)
diffNW_5_10=(1.65+2.74*x5)*10.^-6*exp(-16600/8.314/283)
diffNW_5_20=(1.65+2.74*x5)*10.^-6*exp(-16600/8.314/293)
diffNW_6_0=(1.65+2.74*x6)*10.^-6*exp(-16600/8.314/273)
diffNW_6_10=(1.65+2.74*x6)*10.^-6*exp(-16600/8.314/283)
diffNW_6_20=(1.65+2.74*x6)*10.^-6*exp(-16600/8.314/293)
DNW=[
diffNW_1_0
diffNW_2_0
diffNW_5_0
diffNW_6_0
diffNW_1_10
diffNW_2_10
diffNW_5_10
diffNW_6_10
diffNW_1_20
diffNW_2_20
```

```
diffNW_5_20

diffNW_6_20]
```

F. Enhancement factor calculation

```
function reaction=Enhance(n)

global m q  EnhanceFactor

t = 1.0 ;

[ m , q ] = calculate_these ( t ) ;

nmesh = 21;

nplot = nmesh ;

x = linspace (0, 1, nmesh ) ;

solinit =bvpinit ( x , @guess );

sol = bvp4c (@odes, @bcs, solinit);

y = deval(sol, x)

y(1,:);

y(3,:);

EnhanceFactor = y(2,1);

EnhanceFactor

Hatta=m;


function yinit = guess (x)

global m q bi_gas

y1= exp(-m*x);

y2= 0. * y1;
```

```
yinit = [y1
y2
y2
y2] ;
function dydx = odes ( x, y )
6
global m q bi_gas
dydx = [ y(2)
(m^2 * y(1)* y(3) )
y(4)
(m)^2 * y(1)* y(3)/q ] ;
function res = bcs ( ya , yb)
global n i
i=1-0.001*n+0.001;
res = [ (ya(1)-i)
(ya(4))
(yb(1) )
(yb(3) -1) ] ;
function [ m , q  ] = calculate_these ( t )
global DCN DNW CNH3 kL CCO2 MNH3
da =DCN(MNH3,1);
k2= 0.8;
db = DNW(MNH3,1) ;
astar =CCO2 ;
msq = da.*k2.*CNH3./kL.^2;
```

```
m = msq.^(0.5);

db = DNW(MNH3,1);

z = 1. ;

q = db .* CNH3 ./ ( z .* da.* astar );
```

G. Iteration calculation for enhancement factor for various ammonia and sulfur dioxide concentration

a. NH_3= 6M

```
global SOin EnhanceFactor yr1s ydiffcabsmin mC_1 CNH3 kL kLCN T CO2 n


n=1

CNH3=6000%mol/m3

CO2=2.0

T=273

property

reaction

Emat=EnhanceFactor

SOin=[500];%ppm

CNH3=6000%mol/m3

CO2=2.0
```

```
T=273

Tryy1

Emat=[Emat;EnhanceFactor]

Eslo=yr1s(ydiffcabsmin)

SOin=[1000];%ppm

CNH3=6000%mol/m3

CO2=2.0

T=273

Tryy1

Emat=[Emat;EnhanceFactor]

SOin=[1500];%ppm

CNH3=6000%mol/m3

CO2=2.0

T=273

Tryy1

Emat=[Emat;EnhanceFactor]

SOin=[2000];%ppm

CNH3=6000%mol/m3

CO2=2.0

T=273

Tryy1

Emat=[Emat;EnhanceFactor]

SOin=[2500];%ppm

CNH3=6000%mol/m3

CO2=2.0
```

```
T=273

Tryy1

Emat=[Emat;EnhanceFactor]

SOin=[3000];%ppm

CNH3=6000%mol/m3

CO2=2.0

T=273

Tryy1

Emat=[Emat;EnhanceFactor]

SOin=[3500];%ppm

CNH3=6000%mol/m3

CO2=2.0

T=273

Tryy1

Emat=[Emat;EnhanceFactor]

SOin=[4000];%ppm

CNH3=6000%mol/m3

CO2=2.0

T=273

Tryy1

Emat=[Emat;EnhanceFactor]


NCO2=-Emat.*kL.*CCO2*10.^(-4)%mol cm-2 s-1

NCO2=NCO2.*10^7% 10-7 cm-2 s-1
```

```
function reaction=Enhance(n)

% program calculates the concentration profiles for gas A

% and liquid reactant B in the film.

% 11-1-03 P. A. Ramachandran

global m q  EnhanceFactor

% The dimensionless parameters are calculated in a separate function.

% m = Hatta number, q = q parameter, bi_Gas = Biot number for gas.

t = 1.0 ; % a dummy parameter

[ m , q ] = calculate_these ( t ) ;

% numerical solution.

nmesh = 21; % intial mesh

nplot = nmesh ; % meshes for plotting the result.

% solution block.

x = linspace (0, 1, nmesh ) ;

solinit =bvpinit ( x , @guess ); % trial solution generated by guess
function

sol = bvp4c (@odes, @bcs, solinit); % bvp solved,

y = deval(sol, x) ;

y(1,:); % concentration profiles displayed

y(3,:); % concentration profile of B

EnhanceFactor = y(2,1);

EnhanceFactor

Hatta=m;


%_____________________________________________________
```

```
function yinit = guess (x)

global m q bi_gas

y1= exp(-m*x);

y2= 0. * y1;

yinit = [y1

y2

y2

y2] ; % some arbitrary guess values here

%-------------------------------------------------------

function dydx = odes ( x, y )

6

global m q bi_gas

dydx = [ y(2)

(m^2 * y(1)* y(3) )

y(4)

(m)^2 * y(1)* y(3)/q ] ;

%-------------------------------------------------------------

function res = bcs ( ya , yb)

global n i

i=1-0.001*n+0.001;

% This is set up for na gas film resistance.

res = [ (ya(1)-i)

(ya(4))

(yb(1) )

(yb(3) -1) ] ;
```

```
%_____________________________________________________________________

function [ m , q  ] = calculate_these ( t )

global DCN DNW CNH3 kL CCO2 MNH3

da =DCN(MNH3,1);

k2= 0.8;

db = DNW(MNH3,1) ;

astar =CCO2 ;

msq = da.*k2.*CNH3./kL.^2;

m = msq.^(0.5);

db = DNW(MNH3,1);

z = 1. ;

q = db .* CNH3 ./ ( z .* da.* astar );









global DSN DCN DNW xr1 yr1 yr1s xr yr ypi EnhanceFactor i n SOin
ydiffcabsmin CCO2 CNH3 kL kLCN T CO2 MNH3

diffuNW;

diffuCN;

DiffuSN;

rS=DSN./DCN;
```

```
rA=DNW./DCN;

SOin=SOin*1.2/1000;

mS_n=2*SOin(1,1)/1000;

mS_n=vpa(mS_n,10);

klCW=9.41*10^(-7)*230^0.65;

kLCN=klCW*(1./rA).^0.66;

if CNH3==2500

    MNH3=2

else

    MNH3=CNH3/1000

end

kL=kLCN(MNH3,1)

HCO2=2.4*10^-2*exp(2400*(1./T-1/298.15));%adjusted by temp

PCO2=CO2*0.01*101325/1000;

CCO2=PCO2*HCO2*1000/101325*1000;

mC=CCO2/CNH3

xr=[0:0.000001:0.4];

yr=1+rS(1,1)*mS_n./mC-(1+rS(1,1)*mS_n./mC+rA(1,1)./mC)*xr;

k=find( yr>0 & yr<1);

yr1=yr(k)

xr1=vpa(xr(k),10);

ypi=1-yr1

ypi=-ypi'

xr1=xr1'

size(ypi)
```

```
size(xr1)
ypi=ypi./xr1
reaction;
ypiabs=abs(ypi-EnhanceFactor)
ypiabsmin=find(ypiabs<50)
ypi(ypiabsmin)
yr1s=yr1(ypiabsmin)
ydiffcabs=abs(yr1s-i)
min(ydiffcabs)

while min(ydiffcabs)>0.001
    n=n+1
    reaction
    ypiabs=abs(ypi-EnhanceFactor)
ypiabsmin=find(ypiabs<50)
ypi(ypiabsmin)
yr1s=yr1(ypiabsmin)
ydiffcabs=abs(yr1s-i)
min(ydiffcabs)

    if n>5000
        break
    end
end
ydiffcabsmin=find(ydiffcabs==min(ydiffcabs))
```

```
yr1s(ydiffcabsmin)

EnhanceFactor

ypi(ypiabsmin(ydiffcabsmin))

i

Erro=min(ydiffcabs)%
```

b. NH_3= 5M

```
global SOin EnhanceFactor yr1s ydiffcabsmin mC_1 CNH3 kL kLCN T CO2 n


n=1

CNH3=5000%mol/m3

CO2=2.0

T=273

property

reaction

Emat=EnhanceFactor

SOin=[500];%ppm

CNH3=5000%mol/m3

CO2=2.0

T=273

Tryy1

Emat=[Emat;EnhanceFactor]

Eslo=yr1s(ydiffcabsmin)
```

```
SOin=[1000];%ppm
CNH3=5000%mol/m3
CO2=2.0
T=273
Tryy1
Emat=[Emat;EnhanceFactor]
SOin=[1500];%ppm
CNH3=6000%mol/m3
CO2=2.0
T=273
Tryy1
Emat=[Emat;EnhanceFactor]
SOin=[2000];%ppm
CNH3=5000%mol/m3
CO2=2.0
T=273
Tryy1
Emat=[Emat;EnhanceFactor]
SOin=[2500];%ppm
CNH3=5000%mol/m3
CO2=2.0
T=273
Tryy1
Emat=[Emat;EnhanceFactor]
SOin=[3000];%ppm
```

```
CNH3=5000%mol/m3

CO2=2.0

T=273

Tryy1

Emat=[Emat;EnhanceFactor]

SOin=[3500];%ppm

CNH3=5000%mol/m3

CO2=2.0

T=273

Tryy1

Emat=[Emat;EnhanceFactor]

SOin=[4000];%ppm

CNH3=5000%mol/m3

CO2=2.0

T=273

Tryy1

Emat=[Emat;EnhanceFactor]


NCO2=-Emat.*kL.*CCO2*10.^(-4)%mol cm-2 s-1

NCO2=NCO2.*10^7% 10-7 cm-2 s-1


function reaction=Enhance(n)

% program calculates the concentration profiles for gas A

% and liquid reactant B in the film.
```

```
% 11-1-03 P. A. Ramachandran

global m q  EnhanceFactor

% The dimensionless parameters are calculated in a separate function.

% m = Hatta number, q = q parameter, bi_Gas = Biot number for gas.

t = 1.0 ; % a dummy parameter

[ m , q ] = calculate_these ( t ) ;

% numerical solution.

nmesh = 21; % intial mesh

nplot = nmesh ; % meshes for plotting the result.

% solution block.

x = linspace (0, 1, nmesh ) ;

solinit =bvpinit ( x , @guess ); % trial solution generated by guess
function

sol = bvp4c (@odes, @bcs, solinit); % bvp solved,

y = deval(sol, x) ;

y(1,:); % concentration profiles displayed

y(3,:); % concentration profile of B

EnhanceFactor = y(2,1);

EnhanceFactor

Hatta=m;


%_____________________________________________________

function yinit = guess (x)

global m q bi_gas

y1= exp(-m*x);
```

```
y2= 0. * y1;

yinit = [y1

y2

y2

y2] ; % some arbitrary guess values here

%-------------------------------------------------------

function dydx = odes ( x, y )

6

global m q bi_gas

dydx = [ y(2)

(m^2 * y(1)* y(3) )

y(4)

(m)^2 * y(1)* y(3)/q ] ;

%-------------------------------------------------------------

function res = bcs ( ya , yb)

global n i

i=1-0.001*n+0.001;

% This is set up for na gas film resistance.

res = [ (ya(1)-i)

(ya(4))

(yb(1) )

(yb(3) -1) ] ;

%_____________________________________________________________________

function [ m , q  ] = calculate_these ( t )

global DCN DNW CNH3 kL CCO2 MNH3
```

```
da =DCN(MNH3,1);

k2= 0.8;

db = DNW(MNH3,1) ;

astar =CCO2 ;

msq = da.*k2.*CNH3./kL.^2;

m = msq.^(0.5);

db = DNW(MNH3,1);

z = 1. ;

q = db .* CNH3 ./ ( z .* da.* astar );
```

```
global DSN DCN DNW xr1 yr1 yr1s xr yr ypi EnhanceFactor i n SOin
ydiffcabsmin CCO2 CNH3 kL kLCN T CO2 MNH3

diffuNW;

diffuCN;

DiffuSN;

rS=DSN./DCN;

rA=DNW./DCN;

SOin=SOin*1.2/1000;

mS_n=2*SOin(1,1)/1000;
```

```
mS_n=vpa(mS_n,10);

klCW=9.41*10^(-7)*230^0.65;

kLCN=klCW*(1./rA).^0.66;

if CNH3==2500

    MNH3=2

else

    MNH3=CNH3/1000

end

kL=kLCN(MNH3,1)

HCO2=2.4*10^-2*exp(2400*(1./T-1/298.15));%adjusted by temp

PCO2=CO2*0.01*101325/1000;

CCO2=PCO2*HCO2*1000/101325*1000;

mC=CCO2/CNH3

xr=[0:0.000001:0.4];

yr=1+rS(1,1)*mS_n./mC-(1+rS(1,1)*mS_n./mC+rA(1,1)./mC)*xr;

k=find( yr>0 & yr<1);

yr1=yr(k)

xr1=vpa(xr(k),10);

ypi=1-yr1

ypi=-ypi'

xr1=xr1'

size(ypi)

size(xr1)

ypi=ypi./xr1

reaction;
```

```
ypiabs=abs(ypi-EnhanceFactor)
ypiabsmin=find(ypiabs<40)
ypi(ypiabsmin)
yr1s=yr1(ypiabsmin)
ydiffcabs=abs(yr1s-i)
min(ydiffcabs)


while min(ydiffcabs)>0.001
    n=n+1
    reaction
    ypiabs=abs(ypi-EnhanceFactor)
ypiabsmin=find(ypiabs<40)
ypi(ypiabsmin)
yr1s=yr1(ypiabsmin)
ydiffcabs=abs(yr1s-i)
min(ydiffcabs)


    if n>5000
        break
    end
end
ydiffcabsmin=find(ydiffcabs==min(ydiffcabs))
yr1s(ydiffcabsmin)
EnhanceFactor
ypi(ypiabsmin(ydiffcabsmin))
```

```
i

Erro=min(ydiffcabs)%
```

c. NH_3= 2.5M

```
global SOin EnhanceFactor yr1s ydiffcabsmin mC_1 CNH3 kL kLCN T CO2 n


n=1

CNH3=2500%mol/m3

CO2=2.0

T=273

property

reaction

Emat=EnhanceFactor

SOin=[500];%ppm

CNH3=2500%mol/m3

CO2=2.0

T=273

Tryy1

Emat=[Emat;EnhanceFactor]

Eslo=yr1s(ydiffcabsmin)

SOin=[1000];%ppm

CNH3=2500%mol/m3

CO2=2.0

T=273

Tryy1

Emat=[Emat;EnhanceFactor]
```

```
SOin=[1500];%ppm
CNH3=2500%mol/m3
CO2=2.0
T=273
Tryy1
Emat=[Emat;EnhanceFactor]
SOin=[2000];%ppm
CNH3=2500%mol/m3
CO2=2.0
T=273
Tryy1
Emat=[Emat;EnhanceFactor]
SOin=[2500];%ppm
CNH3=2500%mol/m3
CO2=2.0
T=273
Tryy1
Emat=[Emat;EnhanceFactor]
SOin=[3000];%ppm
CNH3=2500%mol/m3
CO2=2.0
T=273
Tryy1
Emat=[Emat;EnhanceFactor]
SOin=[3500];%ppm
```

```
CNH3=2500%mol/m3

CO2=2.0

T=273

Tryy1

Emat=[Emat;EnhanceFactor]

SOin=[4000];%ppm

CNH3=2500%mol/m3

CO2=2.0

T=273

Tryy1

Emat=[Emat;EnhanceFactor]


NCO2=-Emat.*kL.*CCO2*10.^(-4)%mol cm-2 s-1

NCO2=NCO2.*10^7% 10-7 cm-2 s-1


function reaction=Enhance(n)

% program calculates the concentration profiles for gas A

% and liquid reactant B in the film.

% 11-1-03 P. A. Ramachandran

global m q  EnhanceFactor

% The dimensionless parameters are calculated in a separate function.

% m = Hatta number, q = q parameter, bi_Gas = Biot number for gas.

t = 1.0 ; % a dummy parameter

[ m , q ] = calculate_these ( t ) ;
```

```
% numerical solution.

nmesh = 21; % intial mesh

nplot = nmesh ; % meshes for plotting the result.

% solution block.

x = linspace (0, 1, nmesh ) ;

solinit =bvpinit ( x , @guess ); % trial solution generated by guess
function

sol = bvp4c (@odes, @bcs, solinit); % bvp solved,

y = deval(sol, x) ;

y(1,:); % concentration profiles displayed

y(3,:); % concentration profile of B

EnhanceFactor = y(2,1);

EnhanceFactor

Hatta=m;


%_____________________________________________________

function yinit = guess (x)

global m q bi_gas

y1= exp(-m*x);

y2= 0. * y1;

yinit = [y1

y2

y2

y2] ; % some arbitrary guess values here

%-------------------------------------------------------
```

```
function dydx = odes ( x, y )

6

global m q bi_gas

dydx = [ y(2)

(m^2 * y(1)* y(3) )

y(4)

(m)^2 * y(1)* y(3)/q ] ;

%-------------------------------------------------------------

function res = bcs ( ya , yb)

global n i

i=1-0.001*n+0.001;

% This is set up for na gas film resistance.

res = [ (ya(1)-i)

(ya(4))

(yb(1) )

(yb(3) -1) ] ;

%_____________________________________________________________________

function [ m , q  ] = calculate_these ( t )

global DCN DNW CNH3 kL CCO2 MNH3

da =DCN(MNH3,1);

k2= 0.8;

db = DNW(MNH3,1) ;

astar =CCO2 ;

msq = da.*k2.*CNH3./kL.^2;

m = msq.^(0.5);
```

```
db = DNW(MNH3,1);

z = 1. ;

q = db .* CNH3 ./ ( z .* da.* astar );




global DSN DCN DNW xr1 yr1 yr1s xr yr ypi EnhanceFactor i n SOin
ydiffcabsmin CCO2 CNH3 kL kLCN T CO2 MNH3

diffuNW;

diffuCN;

DiffuSN;

rS=DSN./DCN;

rA=DNW./DCN;

SOin=SOin*1.2/1000;

mS_n=2*SOin(1,1)/1000;

mS_n=vpa(mS_n,10);

klCW=9.41*10^(-7)*230^0.65;

kLCN=klCW*(1./rA).^0.66;

if CNH3==2500

    MNH3=2

else

    MNH3=CNH3/1000

end

kL=kLCN(MNH3,1)

HCO2=2.6*10^-2*exp(2400*(1./T-1/298.15));%adjusted by temp
```

```
PCO2=CO2*0.01*101325/1000;

CCO2=PCO2*HCO2*1000/101325*1000;

mC=CCO2/CNH3

xr=[0:0.0000001:0.4];

yr=1+rS(1,1)*mS_n./mC-(1+rS(1,1)*mS_n./mC+rA(1,1)./mC)*xr;

k=find( yr>0 & yr<1);

yr1=yr(k)

xr1=vpa(xr(k),10);

ypi=1-yr1

ypi=-ypi'

xr1=xr1'

size(ypi)

size(xr1)

ypi=ypi./xr1

reaction;

ypiabs=abs(ypi-EnhanceFactor)

ypiabsmin=find(ypiabs<18)

ypi(ypiabsmin)

yr1s=yr1(ypiabsmin)

ydiffcabs=abs(yr1s-i)

min(ydiffcabs)


while min(ydiffcabs)>0.01

    n=n+1

    reaction
```

```
    ypiabs=abs(ypi-EnhanceFactor)
ypiabsmin=find(ypiabs<18)
yr1s=yr1(ypiabsmin)
ydiffcabs=abs(yr1s-i)
min(ydiffcabs)

    if n>5000
        break
    end
end
ydiffcabsmin=find(ydiffcabs==min(ydiffcabs))
yr1s(ydiffcabsmin)
EnhanceFactor
ypi(ypiabsmin(ydiffcabsmin))
i
Erro=min(ydiffcabs)%
```

d. NH_3= 1M

```
global SOin EnhanceFactor yr1s ydiffcabsmin mC_1 CNH3 kL kLCN T CO2 n

n=1
CNH3=1000%mol/m3
CO2=2.0
```

T=273

property

reaction

Emat=EnhanceFactor

SOin=[500];%ppm

CNH_3=1000%mol/m3

CO_2=2.0

T=273

Tryy1

Emat=[Emat;EnhanceFactor]

Eslo=yr1s(ydiffcabsmin)

SOin=[1000];%ppm

CNH_3=1000%mol/m3

CO_2=2.0

T=273

Tryy1

Emat=[Emat;EnhanceFactor]

SOin=[1500];%ppm

CNH_3=1000%mol/m3

CO_2=2.0

T=273

Tryy1

Emat=[Emat;EnhanceFactor]

SOin=[2000];%ppm

CNH_3=1000%mol/m3

```
CO2=2.0
T=273
Tryy1
Emat=[Emat;EnhanceFactor]
SOin=[2500];%ppm
CNH3=1000%mol/m3
CO2=2.0
T=273
Tryy1
Emat=[Emat;EnhanceFactor]
SOin=[3000];%ppm
CNH3=1000%mol/m3
CO2=2.0
T=273
Tryy1
Emat=[Emat;EnhanceFactor]
SOin=[3500];%ppm
CNH3=1000%mol/m3
CO2=2.0
T=273
Tryy1
Emat=[Emat;EnhanceFactor]
SOin=[4000];%ppm
CNH3=1000%mol/m3
CO2=2.0
```

```
T=273

Tryy1

Emat=[Emat;EnhanceFactor]


NCO2=-Emat.*kL.*CCO2*10.^(-4)%mol cm-2 s-1

NCO2=NCO2.*10^7% 10-7 cm-2 s-1


function reaction=Enhance(n)

% program calculates the concentration profiles for gas A

% and liquid reactant B in the film.

% 11-1-03 P. A. Ramachandran

global m q  EnhanceFactor

% The dimensionless parameters are calculated in a separate function.

% m = Hatta number, q = q parameter, bi_Gas = Biot number for gas.

t = 1.0 ; % a dummy parameter

[ m , q ] = calculate_these ( t ) ;

% numerical solution.

nmesh = 21; % intial mesh

nplot = nmesh ; % meshes for plotting the result.

% solution block.

x = linspace (0, 1, nmesh ) ;

solinit =bvpinit ( x , @guess ); % trial solution generated by guess
function

sol = bvp4c (@odes, @bcs, solinit); % bvp solved,

y = deval(sol, x) ;
```

```
y(1,:); % concentration profiles displayed

y(3,:); % concentration profile of B

EnhanceFactor = y(2,1);

EnhanceFactor

Hatta=m;


%_____________________________________________________

function yinit = guess (x)

global m q bi_gas

y1= exp(-m*x);

y2= 0. * y1;

yinit = [y1

y2

y2

y2] ; % some arbitrary guess values here

%-------------------------------------------------------

function dydx = odes ( x, y )

6

global m q bi_gas

dydx = [ y(2)

(m^2 * y(1)* y(3) )

y(4)

(m)^2 * y(1)* y(3)/q ] ;

%-------------------------------------------------------------

function res = bcs ( ya , yb)
```

```
global n i

i=1-0.001*n+0.001;

% This is set up for na gas film resistance.

res = [ (ya(1)-i)

(ya(4))

(yb(1) )

(yb(3) -1) ] ;

%_____________________________________________________________________

function [ m , q  ] = calculate_these ( t )

global DCN DNW CNH3 kL CCO2 MNH3

da =DCN(MNH3,1);

k2= 0.8;

db = DNW(MNH3,1) ;

astar =CCO2 ;

msq = da.*k2.*CNH3./kL.^2;

m = msq.^(0.5);

db = DNW(MNH3,1);

z = 1. ;

q = db .* CNH3 ./ ( z .* da.* astar );
```

```
global DSN DCN DNW xr1 yr1 yr1s xr yr ypi EnhanceFactor i n SOin
ydiffcabsmin CCO2 CNH3 kL kLCN T CO2 MNH3

diffuNW;

diffuCN;

DiffuSN;

rS=DSN./DCN;

rA=DNW./DCN;

SOin=SOin*1.2/1000;

mS_n=2*SOin(1,1)/1000;

mS_n=vpa(mS_n,10);

klCW=9.41*10^(-7)*230^0.65;

kLCN=klCW*(1./rA).^0.66;

if CNH3==2500

    MNH3=2

else

    MNH3=CNH3/1000

end

kL=kLCN(MNH3,1)

HCO2=2.4*10^-2*exp(2400*(1./T-1/298.15));%adjusted by temp

PCO2=CO2*0.01*101325/1000;

CCO2=PCO2*HCO2*1000/101325*1000;

mC=CCO2/CNH3

xr=[0:0.000001:0.4];

yr=1+rS(1,1)*mS_n./mC-(1+rS(1,1)*mS_n./mC+rA(1,1)./mC)*xr;
```

```
k=find( yr>0 & yr<1);

yr1=yr(k)

xr1=vpa(xr(k),10);

ypi=1-yr1

ypi=-ypi'

xr1=xr1'

size(ypi)

size(xr1)

ypi=ypi./xr1

reaction;

ypiabs=abs(ypi-EnhanceFactor)

ypiabsmin=find(ypiabs<50)

ypi(ypiabsmin)

yr1s=yr1(ypiabsmin)

ydiffcabs=abs(yr1s-i)

min(ydiffcabs)


while min(ydiffcabs)>0.001

    n=n+1

    reaction

    ypiabs=abs(ypi-EnhanceFactor)

ypiabsmin=find(ypiabs<50)

ypi(ypiabsmin)

yr1s=yr1(ypiabsmin)

ydiffcabs=abs(yr1s-i)
```

```
min(ydiffcabs)


    if n>5000
        break
    end
end
ydiffcabsmin=find(ydiffcabs==min(ydiffcabs))
yr1s(ydiffcabsmin)
EnhanceFactor
ypi(ypiabsmin(ydiffcabsmin))
i
Erro=min(ydiffcabs)%
```

B. Appendix B- Analytical solution of mass transfer of CO_2 in ammonia

According to the model shown in Figure 5-1, there is no reaction in Region I. Thus, the right side of (5-9) to (5-11) is replaced by 0

$$D_{\mathrm{CO_2}} \frac{d^2 C_{CO_2}}{dx^2} = 0 \ \ (0 < \mathrm{x} < x_r) \tag{B-1}$$

$$D_{SO_2} \frac{d^2 C_{SO_2}}{dx^2} = 0 (0 < \mathrm{x} < x_r) \tag{B-2}$$

$$D_{NH_3} \frac{d^2 C_{NH_3}}{dx^2} = 0 \ \ (0 < \mathrm{x} < x_r) \tag{B-3}$$

$$D_{\mathrm{CO_2}} \frac{d^2 C_{CO_2}}{dx^2} = k_{CO_2} C_{CO_2} C_{NH_3} \ \ (x_r < \mathrm{x} < x_f) \tag{B-4}$$

$$D_{NH_3} \frac{d^2 C_{NH_3}}{dx^2} = k_{CO_2} C_{CO_2} C_{NH_3} \ \ (x_r < \mathrm{x} < x_f) \tag{B-5}$$

The boundary conditions are:

x=0 $\quad C_{CO_2}$=C_0, $C_{SO_2} = S_0$ (B-6)

x=x_r $\quad C_{CO_2} = C_r$, $C_{SO_2} = 0$, $C_{NH_3} = 0$, $-v_B D_{SO_2} \left(\frac{dC_{SO_2}}{dx}\right) = D_{NH_3} (\frac{dC_{NH_3}}{dx})$ (B-7)

x=x_f $\quad C_{CO_2}$=0, $C_{SO_2} = 0$, $C_{NH_3} = A_0$ (B-8)

The enhancement factor E for carbon dioxide mass transfer, defined as the ratio of molar flux with the chemical reaction to that obtained without the chemical reaction, are as follows:

Mass flux without chemical reaction

$$J_{CO_2-diffusion} = -D_{CO_2}\frac{dC_{CO_2}}{dx} \quad \text{(B-9)}$$

Mass flux with chemical reaction

$$J_{CO_2-reaction} = D_{CO_2}\frac{C_0 - 0}{x_f} \quad \text{(B-10)}$$

$$E_{CO_2} = \frac{J_{CO_2-reaction}}{J_{CO_2-diffusion}} \quad \text{(B-11)}$$

$$E_{CO_2} = -\frac{d\left(\frac{C_{CO_2}}{C_0}\right)}{d\left(\frac{x}{x_f}\right)} \quad \text{(B-12)}$$

The reaction of CO_2 in alkaline system has been classified into a first-order fast reaction with respect to CO_2 and SO_2 into instantaneous reactions[2, 35]. Because the equation (B-1) to (B-5) are nonlinear and cannot be solved analytically, approximate analytical solution was obtained by assuming the concentration of carbon dioxide in region $x_r < x < x_f$ is linear. In Hikita's work[39], the equation was reduced to a form can be solved analytically as follows:

To obtain the relation between carbon dioxide and ammonia, combine equations (B-4) and (B-5):

$$D_{CO_2}\frac{d^2C_{CO_2}}{dx^2} - D_{NH_3}\frac{d^2C_{NH_3}}{dx^2} = 0 \quad \text{(B-13)}$$

Integrating the equation:

$$D_{CO_2}\frac{dC_{CO_2}}{dx} - D_{NH_3}\frac{dC_{NH_3}}{dx} = c_1 \quad \text{(B-14)}$$

$$D_{CO_2}C_{CO_2} - D_{NH_3}C_{NH_3} = c_1 x + c_2 \quad \text{(B-15)}$$

Using boundary conditions (B-7)and (B-8) :

$\text{x} = x_r$: $C_{CO_2} = C_r, C_{NH_3} = 0$ (B-16)

$\text{x} = x_f$: $C_{CO_2} = 0, C_{NH_3} = A_0$ (B-17)

We have:

$$D_{CO_2}C_r = c_1 x_r + c_2 \quad \text{(B-18)}$$

$$-\frac{D_{NH_3}}{v}A_0 = c_1 x_f + c_2 \quad \text{(B-19)}$$

(B-18) - (B-19):

$$D_{CO_2}C_r + \frac{D_{NH_3}}{v}A_0 = c_1(x_r - x_f) \quad \text{(B-20)}$$

$$c_1 = \frac{D_{CO_2}C_r + \frac{D_{NH_3}}{v}A_0}{(x_r - x_f)} \quad \text{(B-21)}$$

Both sides of equation (B-18) divided by x_r :

$$\frac{D_{CO_2}C_r}{x_r} = c_1 + \frac{c_2}{x_r} \tag{B-22}$$

Both sides of equation (B-19) divided byx_f:

$$\frac{-D_{NH_3}C_0}{x_f} = c_1 + \frac{c_2}{x_f} \tag{B-23}$$

(B-22) - (B-23):

$$\frac{D_{CO_2}C_r}{x_r} + \frac{D_{NH_3}A_0}{x_f} = \frac{c_2}{x_r} - \frac{c_2}{x_f} \tag{B-24}$$

$$c_2 = \frac{\frac{D_{CO_2}C_r}{x_r} + \frac{D_{NH_3}A_0}{x_f}}{\frac{1}{x_r} - \frac{1}{x_f}} \tag{B-25}$$

$$c_2 = \frac{D_{CO_2}C_r x_f + D_{NH_3}A_0 x_r}{x_f - x_r} \tag{B-26}$$

Replace the $c_1$and $c_2$in (B-19) with equations (B-21) and (B-26):

$$D_{CO_2}C_{CO_2} - D_{NH_3}C_{NH_3} = \frac{D_{CO_2}C_r + D_{NH_3}A_0}{x_r - x_f}x + \frac{D_{CO_2}C_r x_f + D_{NH_3}A_0 x_r}{x_f - x_r} \tag{B-27}$$

$$(D_{CO_2}C_{CO_2} - D_{NH_3}C_{NH_3})(x_r - x_f) = D_{CO_2}C_r + D_{NH_3}A_0)x - D_{CO_2}C_r x_f - D_{NH_3}A_0 x_r \tag{B-28}$$

$$D_{CO_2}C_{CO_2}x_r - D_{CO_2}C_{CO_2}x_f - D_{NH_3}C_{NH_3}x_r + D_{NH_3}C_{NH_3}x_f = D_{CO_2}C_r x + D_{NH_3}A_0 x - D_{CO_2}C_r x_f - D_{NH_3}A_0 x_r \tag{B-29}$$

Both sides of equation (5-24) divided by D_{CO_2}:

$$C_{CO_2}x_r - C_{CO_2}x_f - \frac{D_{NH_3}}{D_{CO_2}}C_{NH_3}x_r + \frac{D_{NH_3}}{D_{CO_2}}C_{NH_3}x_f = C_r x + \frac{D_{NH_3}}{D_{CO_2}}A_0 x - C_r x_f - \frac{D_{NH_3}}{D_{CO_2}}A_0 x_r \quad \text{(B-30)}$$

Define $\frac{D_{NH_3}}{D_{CO_2}} = r_c$:

$$C_{CO_2}x_r - C_{CO_2}x_f - C_{NH_3}x_r r_c + C_{NH_3}x_f r_c = C_r x + C_0 x r_c - C_r x_f - A_0 x_r r_c \quad \text{(B-31)}$$

Both sides of equation (B-31) divided by x_f:

$$\frac{C_{CO_2}x_r}{x_f} - C_{CO_2} - \frac{C_{NH_3}x_r r_c}{v x_f} + C_{NH_3}r_c = \frac{C_r x}{x_f} + \frac{A_0 x r_c}{x_f} - C_r - \frac{A_0 x_r r_c}{x_f} \quad \text{(B-32)}$$

Assume that the concentration profile of carbon dioxide in the region $0 < x < x_f$ is linear and can be approximated by:

$$C_{CO_2} = \frac{dC_{CO_2}}{dx}(x - x_r) + C_r \quad \text{(B-33)}$$

$$C_{CO_2} = \frac{C_0}{x_f}(x - x_r) + C_r \quad \text{(B-34)}$$

$$\frac{x}{x_f} = 1 - \frac{C_{CO_2}}{C_0} \quad \text{(B-35)}$$

Put equation (B-35) to (B-32) to replace $\frac{x}{x_f}$:

$$\frac{C_{CO_2}x_r}{x_f} - C_{CO_2} - \frac{C_{NH_3}x_r r_c}{x_f} + C_{NH_3}r_c = C_r\left(1 - \frac{C_{CO_2}}{C_0}\right) + A_0 r_c\left(1 - \frac{C_{CO_2}}{C_0}\right) - C_r - \frac{A_0 x_r r_c}{x_f} \quad \text{(B-36)}$$

$$\frac{C_{CO_2}x_r}{x_f} - C_{CO_2} - \frac{C_{NH_3}x_r r_c}{x_f} + C_{NH_3}r_c = -\frac{C_r C_{CO_2}}{C_0} + A_0 r_c - \frac{A_0 r_c C_{CO_2}}{C_0} - \frac{A_0 x_r r_c}{x_f} \quad \text{(B-37)}$$

Define $\frac{x_r}{x_f} = z$

$$C_{CO_2}z - C_{CO_2} - C_{NH_3}zr_c + C_{NH_3}r_c = -\frac{C_r C_{CO_2}}{C_0} + C_0 r_c - \frac{A_0 r_c C_{CO_2}}{C_0} - A_0 \mathrm{z} r_c \quad \text{(B-38)}$$

$$C_{CO_2}z - C_{CO_2} + C_{NH_3}(r_c - zr_c) = -\frac{C_r C_{CO_2}}{C_0} + A_0 r_c - \frac{A_0 r_c C_{CO_2}}{C_0} - A_0 \mathrm{z} r_c \quad \text{(B-39)}$$

$$C_{NH_3}(r_c - zr_c) = C_{CO_2} - C_{CO_2}z - \frac{C_r C_{CO_2}}{C_0} + A_0 r_c - \frac{A_0 r_c C_{CO_2}}{C_0} - A_0 \mathrm{z} r_c \quad \text{(B-40)}$$

$$C_{NH_3}(r_c - zr_c) = C_{CO_2} - C_{CO_2}z - \frac{C_r C_{CO_2}}{C_0} + C_0 r_c - \frac{A_0 r_c C_{CO_2}}{C_0} - A_0 \mathrm{z} r_c \quad \text{(B-41)}$$

$$C_{NH_3} = \frac{C_{CO_2} - C_{CO_2}z - \frac{C_r C_{CO_2}}{C_0} + A_0 r_c - \frac{A_0 r_c C_{CO_2}}{C_0} - A_0 \mathrm{z} r_c}{r_c(1-z)} \quad \text{(B-42)}$$

Define $\frac{A_0}{C_0} = q_c$

$$C_{NH_3} = \frac{\frac{C_{CO_2}A_0}{q_c C_0} - \frac{C_{CO_2}zA_0}{q_c C_0} - \frac{C_r C_{CO_2}A_0}{q_c {C_0}^2} + A_0 r_c - \frac{A_0 r_c C_{CO_2}}{C_0} - A_0 \mathrm{z} r_c}{r_c(1-z)} \quad \text{(B-43)}$$

$$C_{NH_3} = \frac{A_0\left(\frac{C_{CO_2}}{q_c C_0} - \frac{C_{CO_2}z}{q_c C_0} - \frac{C_r C_{CO_2}}{q_c {C_0}^2} + r_c - \frac{r_c C_{CO_2}}{C_0} - \mathrm{z} r_c\right)}{r_c(1-z)} \quad \text{(B-44)}$$

$$C_{NH_3} = A_0 \frac{(C_{CO_2} - C_{CO_2} z - \frac{C_r C_{CO_2}}{C_0} - C_{CO_2} r_c q_c)}{q_c C_0 r_c (1-z)} + A_0 \quad \text{(B-45)}$$

$$C_{NH_3} = A_0 C_{CO_2} \frac{(1 - z - \frac{C_r}{C_0} - r_c q_c)}{q_c C_0 r_c (1-z)} + A_0 \quad \text{(B-46)}$$

$$C_{NH_3} = A_0 C_{CO_2} \left(\frac{1}{q_c C_0 r_c (1-z)\left(1 - \frac{C_r}{C_0}\right)} - \frac{z}{q_c C_0 r_c (1-z)} - \frac{1}{C_0 (1-z)} \right) + A_0 \quad \text{(B-47)}$$

$$C_{NH_3} = A_0 \left(\frac{C_{CO_2} - C_{CO_2} z + \frac{C_{CO_2} C_r z}{C_0} - C_{CO_2} q_c r_c + \frac{q_c r_c C_r C_{CO_2}}{C_0} + q_c C_0 r_c - q_c r_c C_r - q_c r_c C_0 z + q_c r_c C_r z}{q_c C_0 r_c (1-z)\left(1 - \frac{C_r}{C_0}\right)} \right) \quad \text{(B-48)}$$

$\frac{x_r}{x_f}$ can be obtained as follows:

In boundary condition (B-7):

$$-v_B D_{SO_2} \left(\frac{dC_{SO_2}}{dx} \right) = D_{NH_3} \left(\frac{dC_{NH_3}}{dx} \right) \quad \text{(B-49)}$$

Apply equations (B-14)and (B-21) to eliminate $D_{NH_3}(\frac{dC_{NH_3}}{dx})$:

$$-v_B D_{SO_2} \left(\frac{dC_{SO_2}}{dx} \right) = D_{CO_2} \frac{dC_{CO_2}}{dx} - \frac{D_{CO_2} C_r + D_{NH_3} A_0}{(x_r - x_f)} \quad \text{(B-50)}$$

Applying boundary conditions (B-6)and (B-7)to equation (B-2):

$$C_{SO_2} = -\frac{S_0}{x_r} x + S_0 \quad \text{(B-51)}$$

$$\frac{dC_{SO_2}}{dx} = -\frac{S_0}{x_r} \tag{B-52}$$

Apply (B-52) to (B-50) and substitute stoichiometric coefficient 2 and 1 for v_B andv_A:

$$2D_{SO_2}\frac{S_0}{x_r} = C_{CO_2}\frac{dC_{CO_2}}{dx} - \frac{D_{CO_2}C_r + D_{NH_3}A_0}{(x_r - x_f)} \tag{B-53}$$

$$2D_{SO_2}S_0 - 2D_{SO_2}\frac{x_f}{x_r}S_0 = D_{CO_2}1x_r\frac{dC_{CO_2}}{dx} - D_{CO_2}1x_f\frac{dC_{CO_2}}{dx} - 1D_{CO_2}C_r + D_{NH_3}A_0 \tag{B-54}$$

Both sides of equation (B-54) divided byD_{CO_2}:

$$\frac{2D_{SO_2}S_0}{D_{CO_2}} - 2D_{SO_2}\frac{x_f S_0}{x_r D_{CO_2}} = x_r\frac{dC_{CO_2}}{dx} - x_f\frac{dC_{CO_2}}{dx} - C_r + \frac{D_{NH_3}A_0}{D_{CO_2}} \tag{B-55}$$

Define$\frac{D_{SO_2}}{D_{CO_2}} = r_B,\ \frac{D_{NH_3}}{D_{CO_2}} = r_c$:

$$2r_B B_i - v_B\frac{x_f r_B S_0}{x_r} = v_A x_r\frac{dC_{CO_2}}{dx} - v_A x_f\frac{dC_{CO_2}}{dx} - v_A A_r + r_c C_0 \tag{B-56}$$

Both sides of equation (B-56) divided by C_0:

$$\frac{v_B r_B S_0}{C_0} - v_B\frac{x_f r_B}{x_r C_0}S_0 = \frac{x_r dC_{CO_2}}{C_0 dx} - \frac{x_f dC_{CO_2}}{C_0 dx} - \frac{C_r}{C_0} + \frac{r_c A_0}{C_0} \tag{B-57}$$

Define $\frac{2S_0}{C_0} = q_B$:

$$q_B r_B - q_B\frac{x_f r_B}{x_r} = \frac{x_r dC_{CO_2}}{C_0 dx} - \frac{x_f dC_{CO_2}}{C_0 dx} - \frac{C_r}{C_0} + \frac{r_c A_0}{C_0} \tag{B-58}$$

Define $\frac{A_0}{C_0} = q_c$

$$q_B r_B - q_B \frac{x_f r_B}{x_r} = \frac{x_r dC_{CO_2}}{C_0 dx} - \frac{x_f dC_{CO_2}}{C_0 dx} - \frac{C_r}{C_0} + q_c r_c \quad \text{(B-59)}$$

$$q_B r_B - q_B \frac{x_f r_B}{x_r} = \frac{x_r}{x_f}\frac{x_f dC_{CO_2}}{C_0 dx} - \frac{x_f dC_{CO_2}}{C_0 dx} - \frac{C_r}{C_0} + q_c r_c \quad \text{(B-60)}$$

Substitute (B-12) to (B-60):

$$q_B r_B - q_B \frac{x_f r_B}{x_r} = \frac{x_r}{x_f} E_{CO_2} - E_{CO_2} - \frac{C_r}{C_0} + q_c r_c \quad \text{(B-61)}$$

Assume that the concentration profile of carbon dioxide in the region $x_r < x < x_f$ is linear and can be approximated by:

$$C_{CO_2} = \frac{dC_{CO_2}}{dx}(x - x_r) + A_r \quad \text{(B-62)}$$

$$C_{CO_2} = \frac{C_0}{x_f}(x - x_r) + A_r \quad \text{(B-63)}$$

$$C_{CO_2} = \frac{C_0 x}{x_f} - \frac{C_0 x_r}{x_f} + A_r \quad \text{(B-64)}$$

Applying boundary condition (B-8) and have:

$$\frac{x}{x_f} = 1 - \frac{C_{CO_2}}{C_0} \quad \text{(B-65)}$$

$$q_B r_B - q_B \frac{x_f r_B}{x_r} = \frac{x_r}{x_f} E_{CO_2} - E_{CO_2} - 1 - \frac{x_r}{x_f} + q_c r_c \quad \text{(B-66)}$$

$$E_{CO_2} = \frac{[1 + r_B q_B + r_C q_c - (1 + r_b q_B) E_{CO_2}]\gamma\eta}{(1 + r_C q_C - \beta_A)\tanh\gamma\eta} \quad \text{(B-67)}$$

Where γ and η are dimensionless parameters and defined as:

$$\gamma = \left(\frac{kC_0}{D_{CO_2}}\right)^{\frac{1}{2}} \delta \tag{B-68}$$

$$\eta = \frac{1 + r_C q_C - E_{CO_2}}{1 + r_B q_B + r_C q_C - E_{CO_2}} \times \left(\frac{1 + r_B q_B + r_C q_C - (1 + r_B q_B) E_{CO_2}}{3 r_C q_c E_{CO_2}}\right)^{\frac{1}{2}} \tag{B-69}$$

The enhancement factor for B is related with β_A by following equation:

$$E_{SO_2} = \frac{1 + r_B q_B + r_C q_c - E_{CO_2}}{r_B q_B} \tag{B-70}$$

C. Appendix C- Experimental data

C_{CO_2} (ppm)	C_{NH_3}(mol · L^{-1})	$N_{CO_2} \times 10^7$ (mol $cm^{-2}s^{-1}$)	$K_G \times 10^{10}$ (mol pa^{-1} c $m^{-2}s^{-1}$)	$k_{obs} \times 10^3$ (s^{-1})	k_{f1}(m^3mol^{-1} s^{-1})
0	6	2.6649	2.164766777	7.461440026	1.243573338
0	5	2.48534	2.209224501	7.765376975	1.553075395
0	2.5	1.95443	1.329899391	2.816034676	1.12641387
0	1	1.21869	0.735383574	0.860734981	0.860734981
500	1	1.11996	0.618776901	0.608964988	0.608964988
500	2.5	1.70174	1.082693843	1.866430222	0.746572089
500	5	1.74146	1.48383183	3.503097357	0.700619471
500	6	1.7597	1.627903116	4.219466401	0.7032444
1000	1	0.606629	0.308940818	0.151801031	0.151801031
1000	2.5	1.14812	0.63541653	0.642626486	0.257050595
1000	5	1.93427	1.239782976	2.446430831	0.489286166
1000	6	1.96371	1.302224924	2.698080159	0.449680026
1500	1	0.736749	0.380921225	0.230862389	0.230862389
1500	2.5	1.44421	0.823143583	1.078037913	0.431215165
1500	5	2.02438	1.288369994	2.640973507	0.528194701
1500	6	2.1613	1.409501074	3.163233466	0.527205578
2000	1	0.731293	0.378779059	0.228189711	0.228189711
2000	2.5	1.24481	0.682441972	0.740452065	0.296180826
2000	5	1.84849	1.134885705	2.049962212	0.409992442
2000	6	2.13263	1.408177651	3.157296146	0.526216024
3000	5	1.7312	1.039081268	1.718464779	0.343692956
3000	1	0.692656	0.357487378	0.203257024	0.203257024
3000	2.5	1.15987	0.627300569	0.625628975	0.25025159
3000	6	2.10089	1.377485257	3.02116429	0.503527382
4000	5	1.67203	0.992512729	1.567883444	0.313576689
4000	1	0.666015	0.34240283	0.186465645	0.186465645
4000	2.5	1.11241	0.597165039	0.566962376	0.22678495
4000	6	2.07995	1.357499796	2.934134178	0.489022363